

# PLASMONIC PROPERTIES OF LASER ABLATED METAL NANO MATERIALS

## A DISSERTATION

*Submitted in partial fulfillment of the  
requirements for the award of the degree*

*of*

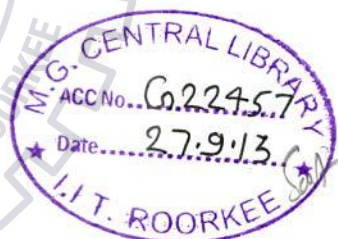
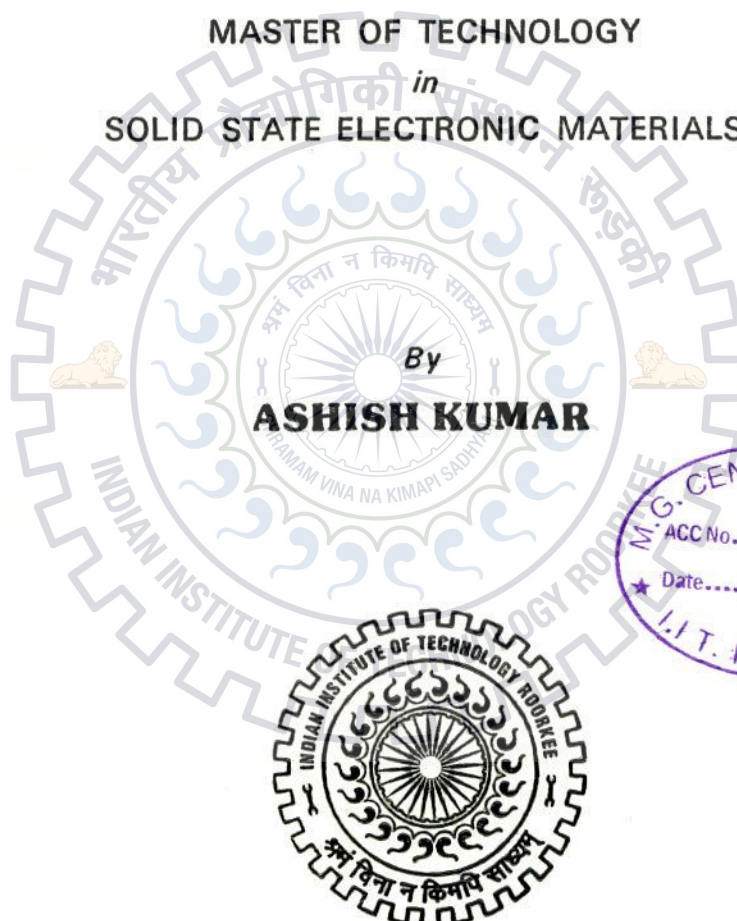
MASTER OF TECHNOLOGY

*in*

SOLID STATE ELECTRONIC MATERIALS

By

**ASHISH KUMAR**



DEPARTMENT OF PHYSICS  
INDIAN INSTITUTE OF TECHNOLOGY ROORKEE  
ROORKEE-247 667 (INDIA)  
JUNE, 2013

## CANDIDATE'S DECLARATION

---

I hereby declare that the work, which is being presented in this Dissertation, entitled "*Plasmonics Properties of Laser Ablated Metal Nanomaterials*" and is being submitted in partial fulfillment of the requirements for the award of degree of Master of Technology in "Solid State Electronic Materials", Indian Institute of Technology, Roorkee, is an authentic record of my own work, carried out under guidance of Dr. Anirban Mitra, Assistant Professor, Department of Physics, Indian Institute of Technology, Roorkee. The results embodied in this report have not been submitted for the award of any other Degree or Diploma.

Date: 14-06-13

Place: Roorkee

*Ashish*

Ashish Kumar

---

## CERTIFICATE

This is to certify that the statement made by the candidate is correct to best of my knowledge and belief.

Date: 14-06-13

Place: Roorkee

*Anirban Mitra*

Dr. Anirban Mitra, Assistant Professor

Department of Physics

IIT Roorkee

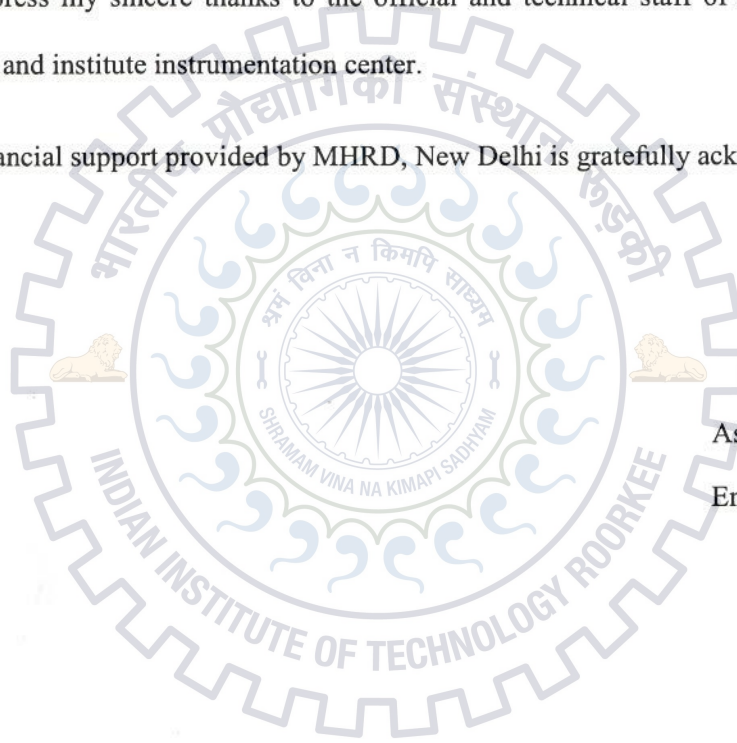
## Acknowledgement

---

I am highly grateful to Dr. Anirban Mitra, Assistant Professor, Department of Physics, IIT Roorkee, for giving his precious time and providing me with a lot of guidance in completing this dissertation report.

I am highly obliged to Prof. A. K. Jain, Head, Department of Physics and Dr. K. L. Yadav course coordinator, M.Tech, for providing the good facilities. I am highly obliged and express my sincere thanks to the official and technical staff of the department of physics and institute instrumentation center.

The financial support provided by MHRD, New Delhi is gratefully acknowledged.



Ashish Kumar

Enroll no- 11550006

## Abstract

This report represents the effective method to enhance surface Plasmon resonance (SPR) on Ag films. Ag films of different thickness are deposited by pulsed laser deposition technique. To enhance surface sensitivity surface plasmons has been used through various spectroscopic measurements such as diffraction, interference and Raman scattering etc. the surface Plasmon resonance (SPR) technique has been employed to characterize optically Ag/glass film of different thickness. The morphology of the film exhibiting SPR responses under different processing condition were analyze by the AFM imaging through ND-MDT machine. The experimental SPR reflectance shows that it is shifted continuously with the increasing number of pulses & decreased with higher number of pulses. Theoretically SPR dip angle were calculated by winspall-302 software. This SPR based system shows a application as a sensors such as biological and chemical sensing application.

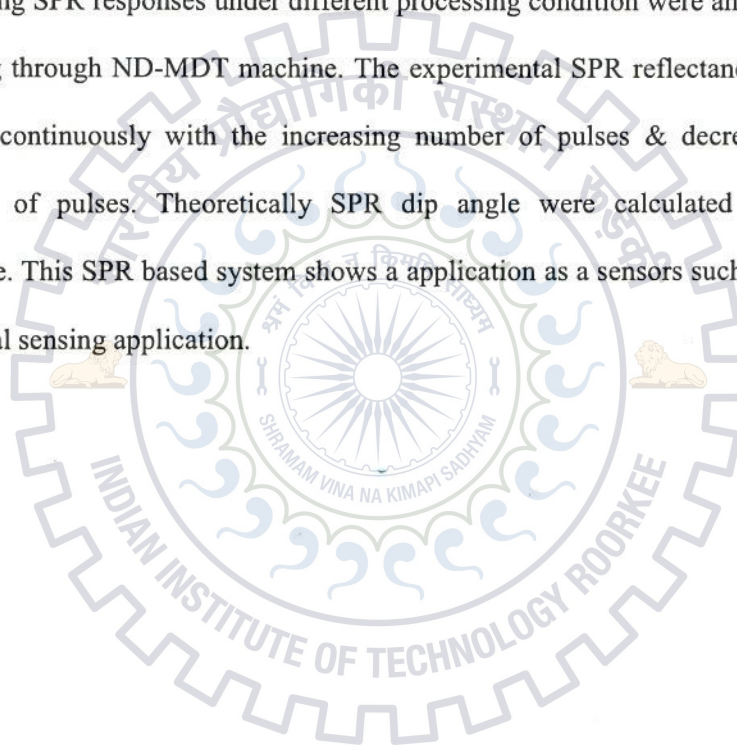


# TABLE OF CONTENTS

<i>Candidate's Declaration</i>	<i>i</i>
<i>Certificate</i>	<i>i</i>
<i>Acknowledgement</i>	<i>ii</i>
<i>Abstract</i>	<i>iii</i>
<i>Table of contents</i>	<i>iv</i>
<i>List of figures</i>	<i>vi</i>
<b>Chapter 1</b>	<b>1</b>
1.1 Introduction	2
<b>Chapter 2</b>	<b>4</b>
2.1 Pulsed Laser deposition and Characterization of Metal Thin Films	4
2.1.1 Introduction	5
2.1.2 Laser Ablation	7
2.1.3 Process Description	7
2.1.4 Plasma Formation and Expansion	8
2.1.5 Advantages of Pulsed Laser Deposition	9
2.1.6 Disadvantages of PLD	9
2.1.7 Applications of PLD	9
2.2 Atomic force Microscopy	10
2.3 Experimental arrangement to observe surface plasmons	
Resonance excitation through prism	14
<b>Chapter 3</b>	<b>16</b>
3.1 Theory of Surface Plasmon of Metal Thin Films	16

3.1.1	Theoretical description	15
3.1.2	Plasmonics	17
3.1.3	Theoretical description on Plasmonics	18
3.1.4	Drude Model	18
3.2	Plasmons	20
3.3	Surface Plasmons	23
3.3.1	The wave equation	25
3.4	Surface Plasmon at Metal Dielectric interface	31
3.5	Surface Plasmons Excitation	36
3.5.1	Prism coupling	38
<b>Chapter 4</b>		41
4.1	Plasmonics Properties of Pulsed Laser Deposited Metal Thin Film	41
4.1.1	Optical Properties	42
4.1.2	Morphology of the film	50
4.2	Conclusion	56
4.3	References	57

## *List of Figures*

- Figure 2.1** Schematic Diagram of Pulsed laser deposition.
- Figure 2.2** Schematic of initial stage of vaporization.
- Figure 2.3** Schematic layout of Atomic force microscope
- Figure 2.4** force versus distance showing the contact, Tapping, and non contact modes
- Figure 2.5** Setup to excite surface Plasmon
- Figure 3.1** Schematic of Drude Model in which electrons are collided between positively charged ions.
- Figure 3.2** Simple diagram of plasma oscillation (a) due to external electric field charges are separated. (b) Without electric field electrons moves back.
- Figure 3.3** Representation of a propagation of electron density wave along a metal-dielectric interface.
- Figure 3.4** Geometry of the planar waveguide.
- Figure 3.5** Schematic of geometry for SPP propagation between metal dielectric interfaces.
- Figure 3.6** Dispersion curves for surface plasmons.
- Figure 3.7** Kretschmann Configuration for attenuated total reflection method
- Figure 3.8** Otto configurations for surface plasmons coupling.
- Figure 4.1** Reflectivity Vs angle of incidence SPR curves of 6000, 70000, 8000, 9000 number of pulses silver films.

- Figure 4.2** Reflectivity Vs angle of incidence SPR curves of 10000, 12000, 14000 number of pulses silver films.
- Figure 4.3** Comparison between experimental and theoretical results for 6000 number of pulses film.
- Figure 4.4** Comparison between experimental and theoretical results for 7000 number of pulses film.
- Figure 4.5** Comparison between experimental and theoretical results for 8000 number of pulses film.
- Figure 4.6** Comparison between experimental and theoretical results for 9000 number of pulses film.
- Figure 4.7** Comparison between experimental and theoretical results for 10000 number of pulses film.
- Figure 4.8** Comparison between experimental and theoretical results for 12000 number of pulses film.
- Figure 4.9** Comparison between experimental and theoretical results for 14000 number of pulses film.
- Figure 4.10 (a)-(g)** AFM images  $1 \times 1 \mu\text{m}^2$  of nano structured silver thin films of 355nm of laser wavelength with their 3-D images of different no. of pulses at room temperature (a)6000 (b)700 (c)8000 (d)9000 (e)10000 (f)12000 (g)14000 number of pulses.
- Figure 4.11** Histogram of AFM shows distribution of particle size of different thickness of silver thin films of 355nm of laser wavelength at room.



# **CHAPTER 1**

## **INTRODUCTION**



## Introduction

The interaction between light and matter is of great importance in the wave range of science and technology. Usually metals are thought just as mirrors, however interaction between light and matter in metals that creates surface plasmons which enable us to use metals more than a mirrors. Surface plasmons are the EM modes from the interaction between light and mobile surface (basically conduction electrons in metals). This interaction leads to surface plasmon resonance mode which are having greater momentum than the momentum of light of the same frequency.

Dealing with the interaction of light with free electron oscillation that propagates along the surface metal that is bound to the dielectric medium constitute the surface plasmons (SP) [1,2] and when the frequency of surface plasmons and the frequency of incident light matches then this condition is known as surface plasmons resonance. It is an optical phenomenon.

Surface plasmons resonance highlights the sensitive detection of optical phenomenon of thin films & interfaces [3] as well as for sensing purpose [4][5]. The evanescent field generated by SPR at the interface of metal/dielectric under total internal reflection condition is the main property of SPR sensors. The strongest effect of evanescent field is due to resonance coupling between surface plasmons wave & incident radiation at the interface of the metal/dielectric. Thus the evanescent field which is associated with interaction decays exponentially in strength with distance from the surface. In the planar surface of metal the surface plasmon modes are bounded to that of surface, propagating and guided by it until their energy is lost as heat in the metals [6].

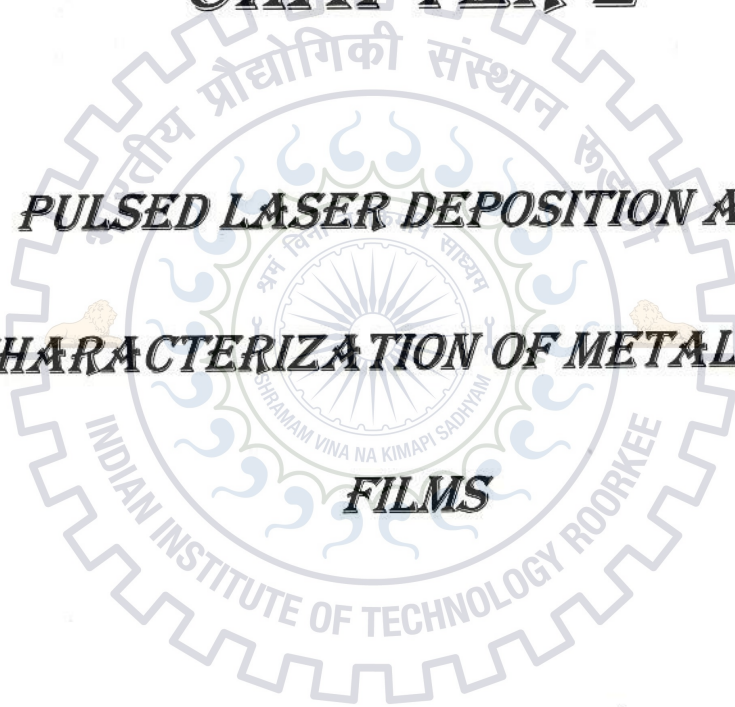
Many fabrication techniques have been applied for the fabrication of Ag film, here we use pulsed laser deposition technique due to the high deposition rate, better film properties, stoichiometric film and process stability.

In this report the experimental result of different deposited film have been investigated by means of the surface plasmon resonance (SPR) technique and morphology of different films were investigated by Atomic force microscopy with the aim to enable the applicability of the SPR based system for the applications of different types of sensors.



# **CHAPTER 2**

## **PULSED LASER DEPOSITION AND CHARACTERIZATION OF METAL THIN FILMS**



## Introduction

Pulsed Laser deposition (PLD) is a thin film deposition technique in which a target in a vacuum chamber is focused by a high energy focused beam. Formation of Plasma plume takes place by the high laser intensities onto the target material which vaporize it and strikes the substrate in the vacuum chamber and the formation of thin film of target material onto the substrate takes place. This deposition technique can be carried out with different types of background gas and under ultra high vacuum.

The significant results of the PLD make the attention in the past few years for its relative use and depositing materials of complex stoichiometry. Among all other techniques, PLD was the first deposition technique used to deposit superconductor YBCO thin film, since at that time various materials are difficult to deposit by the existing deposition techniques but with the pulsed laser technique, deposition of such materials like high temperature superconductors, Ferro electrics and for electro optic materials formation of thin films become easier.

Pulsed laser deposition technique has many applications from integrated circuits(IC) and optoelectronics to micro mechanics and medical applications, and finds applications in device quality functional materials.

From the past few years PLD has been used for the micro and nano structures thin films [7-11]. This techniques has several advantages among all other deposition techniques, the most important advantage is that it retained exact composition as target material and the other advantages are (i) it is a significantly clean process, (ii) it has a high deposition rates.

In the PLD technique, when the high power laser strikes the target, ablation of the target occur and due to this plasma is created this plasma is further in contact with the incoming laser that shields upper surface of the target material that effects the further ablation process. The temperature of the plasma is increased when the plasma from the target material interacts with the incoming laser by absorbing the part of incoming laser radiation. After the termination of pulse plasma plume expands in the vacuum chamber before getting deposited onto the substrate in the vacuum chamber. Therefore there are four sub stages in the PLD process:

- (i) Vaporization of target i.e. Ablation,
- (ii) Formation of the plasma plume,
- (iii) Expansion of the plasma plume,
- (iv) Deposition of the target material at the substrate.

A schematic experimental setup Pulsed Laser Deposition System is shown in **figure 2.1**

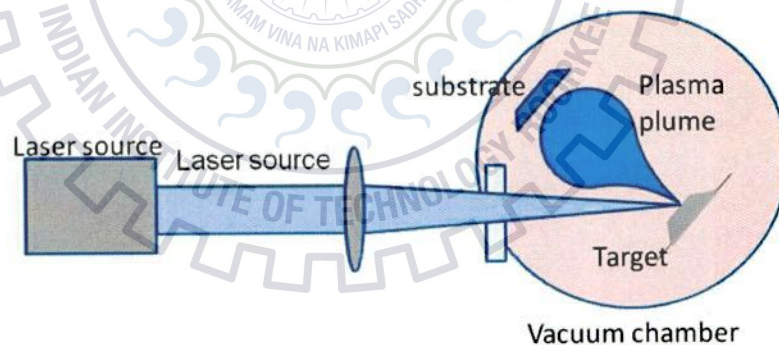


**Fig.2.1** Schematic Diagram of Pulsed laser deposition.

# Laser ablation

## Process Description

When the incoming laser radiation strikes the target surface, a part of the laser radiation is get reflected, while a part of the laser radiation penetrates into the target surface and absorbed by it. The absorbed laser radiation heats the target surface, resulting into melting and evaporation. This constitutes the removal of material as electron gas from the target surface known as laser ablation. Thus there are two stages occur in the laser ablation process.

- (i) Increasing of temperature when the laser radiation absorbed by the target surface. This is shown in **figure 2.2**
- (ii) With the increasing of temperature vaporization occurs that initiates the plasma plume above the surface of the target material.

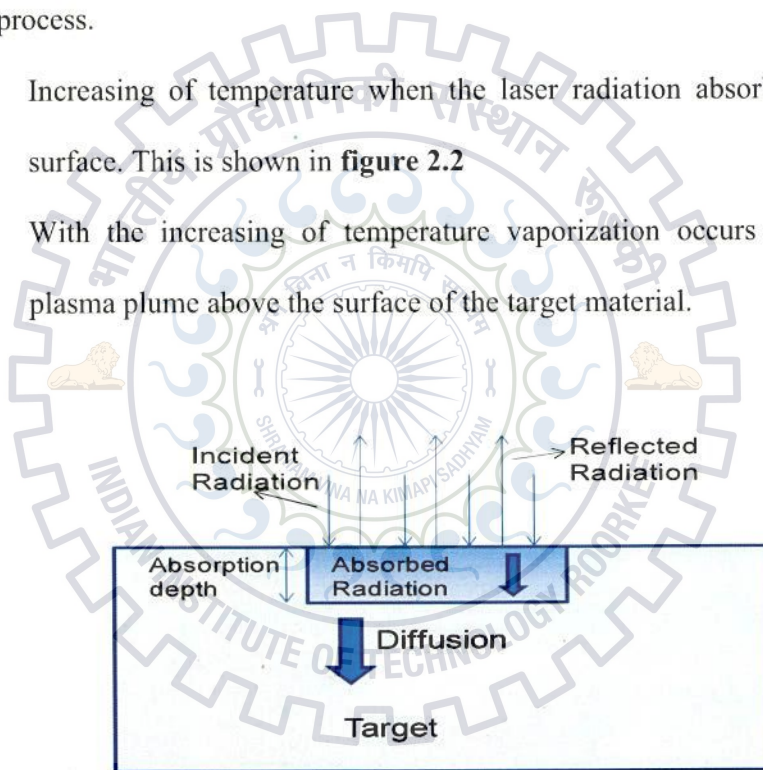


**Figure 2.2** Schematic of initial stage of vaporization.

## Plasma Formation and Expansion

In the mechanism of formation of plasma and expansion in vacuum chamber. During the interaction of the laser radiation and target surface its temperature increases to the critical temperature up to which vaporization occurs and the process of ablation of target surface begins and particles of target surface heated by the incoming laser radiation to form the plasma plume [12], this plasma plume is nothing but a electron gas of target material .

In PLD, the vapours of plasma resulting from the ablation process condense on a substrate to form different structures and of different thickness of thin films. The deposition rate on the substrate is dependent on the rate of plasma plume expansion.

The expansion of the plasma plume is categorized in two stages.

- (i) The heating of the plasma in the presence of the incoming laser radiation.
- (ii) The cooling of the plasma plume and relaxation of the termination of the laser pulse.

The mean thickness of the growth of the film deposited that reaches the state of continuity is given by the expression:

$$N_{99} = A (1/R)^{1/3} \exp (-1/T) \quad (1.1)$$

Where R= Deposition rate

T= Temperature of the substrate

A= Constant related to the materials



### **Advantages of Pulsed Laser Deposition:**

- ❖ Versatile method: Any materials can be grown with different types of background gas with any range of pressure.
- ❖ Congruent evaporation.
- ❖ Simple and clean process: target vaporize with the laser radiation and produce same composition films as target material.
- ❖ Rate of deposition is high
- ❖ High quality film is grown within 5 to 15 mins so this is very fast process.
- ❖ Cost-effectiveness: one laser can serve many vacuums systems.

### **Disadvantages of PLD:**

- ❖ The coverage of film is non conformal.
- ❖ The uniformity area is small.
- ❖ Degradation of target occurs.
- ❖ Creation of particulates.

### **Applications of PLD:**

- ❖ Generation of multilayer films such as superlattice films, heterostructures (e.g. pn junctions) and x-ray mirrors.
- ❖ Generation of ceramics films for example YBCO, SBN, PZT, etc.
- ❖ Hard coating of diamonds/diamonds like films (Tic, Tin, CN, etc).
- ❖ Biomedical devices.
- ❖ Photonics devices.
- ❖ Micro-optics devices.

## Atomic force Microscopy

AFM is a technique used for the study of the surface topography in 3 dimensions i.e. X, Y & Z directions. In this it employs a sharp tip at the cantilever end that moves above the samples in raster scan that crimps in response to the force between the sample and the tip. Earlier, AFM was fitted at the end of the cantilever to monitor its bending. With the STM (scanning tunnelling microscope) and now a day's an optical lever a technique is used for this purpose. This is shown in **figure 2.3** as the light bends from the laser by the cantilever it is gets reflected onto the photodiode. The signal difference is used as a measure of the cantilever and it obeys the hook's laws for small displacement and we get the calculated value of the force between sample and the tip and control the movement of tip or the sample by the device made from piezo-electric ceramic, it is a form of a scanner tube and the resolution of the scanner is up to sub-angstrom level in 3-dimensions i.e. x, y & z directions and z-direction is the perpendicular direction to the sample.

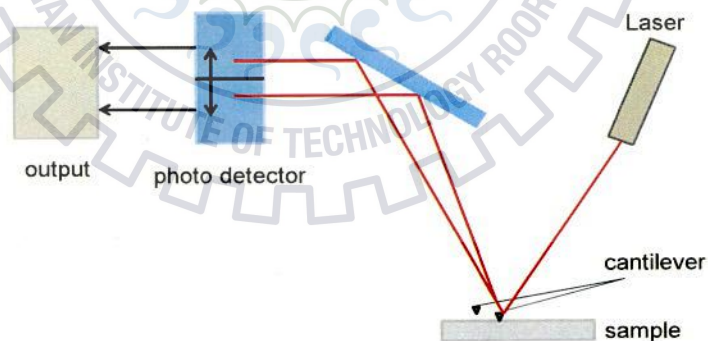


**Figure 2.3** Schematic layout of Atomic force microscope

The operation of the AFM can be done in two modes:

- (i) With feedback control mode

(ii) Or without control mode

In feedback control mode, the force between the tip and the sample is constant in which the sample or tip moves by the Piezo, which responds to any change in the force between the sample and the tip that alters the separations between the two, to restore the original values of the force [32]. This is called as the height measurement mode that helps to know the topographical analysis of the sample.

In without feedback control, the analysis is done at constant height which is also known as deflection mode which is very useful to analyze the sample at high resolution that are extremely flat [33], with the help of this we achieve atomic level resolution that is comprises several refinements such as force feedback, tip-sample positioning at high resolution, sharp tips, flexible cantilever.

Since it employs force of interaction of the atom on the tip to that of the sample [34].

Imaging of the non-conducting samples is also done by the use of AFM.

The measurement of AFM can be done in three modes namely:

- (i) Contact modes
- (ii) Tapping mode
- (iii) Non contact mode

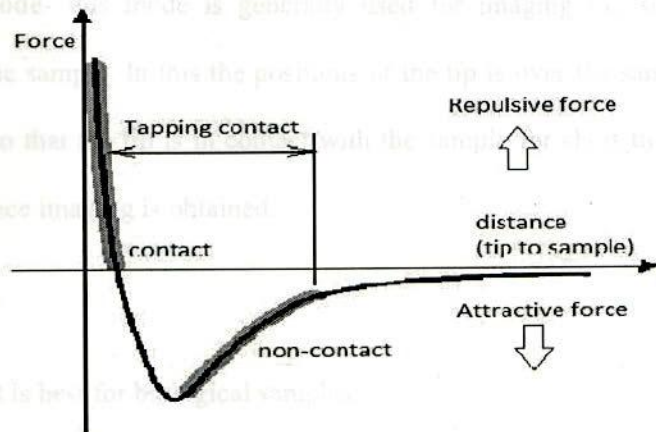


**Figure 2.4** force versus distance showing the contact, Tapping, and non contact modes

**Contact mode-** In this the tip is close in contact with the sample during the scanning process. This method is most commonly used method and there is repulsive force in the intermolecular force curve between the tip and the sample, by the help of this mode we get information in 3-dimensions with 1.5nm lateral and 0.05nm vertical resolution as shown in figure 2.4.

**Advantages**

- (i) It is used in friction analysis.
- (ii) It is good for rough surface.
- (iii) It is fast scanning.

**Disadvantages**

- (i) Soft sample can damage or deform.

**Tapping mode-** this mode is generally used for imaging the soft and immobilised surface of the sample. In this the positions of the tip is over the sample at its resonating frequency, so that the tip is in contact with the sample for short time during oscillation and the surface imaging is obtained.

#### **Advantages**

- (i) It is best for biological samples.
- (ii) It allows high resolution.

#### **Disadvantages**

- (i) Scan speed is slower.
- (ii) Difficult to image in liquids.

**Non-contact mode-** In this mode there is some distance between the tip and the sample so that both are not in contact with each other.

#### **Advantages**

- (i) The lifetime of the probe is long.
- (ii) The force on the sample is very less.

#### **Disadvantages**

- (i) To achieve best imaging, ultra high vacuum (UHV) is needed.
- (ii) Contaminated surface on the sample can interfere with oscillation.
- (iii) It has lower resolution.

In this thesis we uses the contact mode for the AFM imaging, the measurement of the AFM were done on the ND-MDT, NTEGRA.

## Experimental arrangement to observe surface plasmons resonance excitation through prism

The setup shown is based on the krestchmann Reather configuration, which is very most implemented configuration. The schematic diagram of the setup shown in **figure 2.5**.

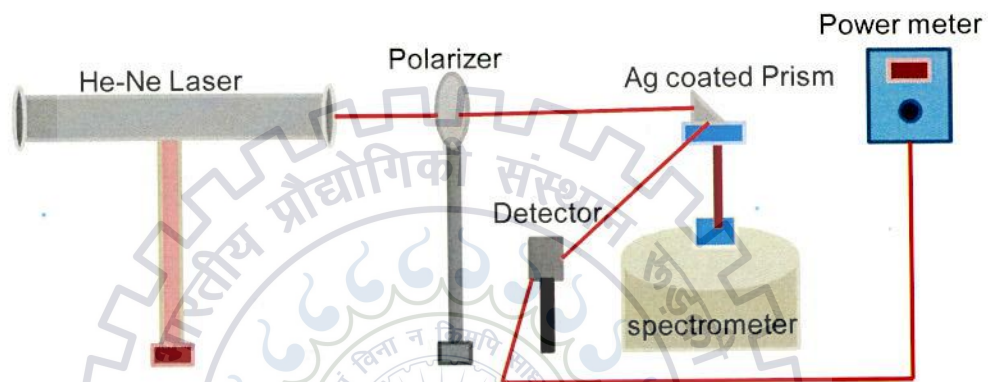


Figure 2.5: Setup to excite surface Plasmon

The beam of Helium-neon (He-Ne) laser (uniphase, 5mW, wavelength ( $\lambda$ ) =632.8nm) passes through a rotating polarizer, by which we get p-polarized light. Now the beam is incident on the prism placed on rotating table. The reflection of laser beam is continuously measured as we vary the incident angle of the laser beam on the prism.

Plasmons resonance coupling will be detected when we noticed a dip in the reflected intensity, because most of the laser power will be transferred through the prism. The reflected beam intensity is measured using a photo diode detector with the help of power meter and measuring the Plasmon coupling angle.

A p-polarized He-Ne laser was used to excite surface plasmons by the prism-coupling technique. The prism was placed on a XYZ $\theta$  rotating stage, intensity of light reflected internally from the metal film was measured with the laser power detector of the resolution of .01 mW at different incident angles near the corresponding SPR dip angles. The measured reflected intensity was divided by the incident intensity of the laser beam to get the reflectance.



## Theoretical description

In this section we describe the theoretical analysis that is necessary to understand the analysis of experimental outcomes.

## Plasmonics

The interaction between incident radiation and conduction electrons in the surface of a metal constitutes the basis of plasmonic processes. These ranges from interface and

Etched surface to size of nanometer scale. This is so called nanostructure. The electromagnetic field produced by large confinement of

dimensions smaller than the wavelength of light. This is called surface plasmon resonance. Interaction between light and surface plasmon resonance.

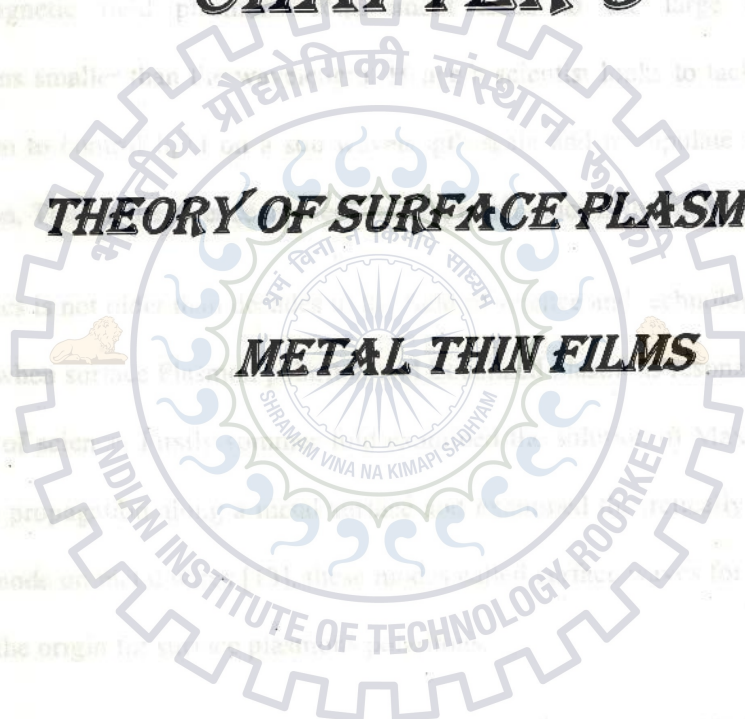
Plasmonics is not only a new technology but also a new science. It is a new picture of surface plasmon resonance. The field of surface plasmon resonance is a new science.

For wave propagation in a medium, the wave vector  $k$  is related to the wave number  $k_0$  by the dispersion relation  $k = k_0 n$ , where  $n$  is the refractive index of the medium. This is the origin of surface plasmon resonance.

Later, Gustav Mie gave the theoretical description for scattering of light on a spherical particle and gave the outline description of localized surface plasmon resonance.

# CHAPTER 3

## THEORY OF SURFACE PLASMON OF METAL THIN FILMS





## Theoretical description

In this section we describe the theoretical analysis that is necessary to understand the analysis of experimental outcomes.

### Plasmonics

The interaction between incident radiation and conduction electrons in the structures of metals constitutes the basis of plasmonics processes. These ranges from interface and Furrowed surface to sizes of nanostructures. This is so called nanostructures, in the electromagnetic field plasmons confinement leads to the large confinement in dimensions smaller than the wavelength. Hence a scientist looks to tackle this resonant interaction to control light on a sub wavelength scale and manipulate light and matter interaction. Thus in the science and technology, plasmonics is the metal based optics.

Plasmonics is not older than decades in the field of science and technology. It comes into pictures when surface Plasmon polariton and Localized plasmons resonance originates in the field of science. Firstly sommer fold examined the solution of Maxwell's equations for wave propagation along a metal surface and examined theoretically electromagnetic surface mode on metal wires [13], these modes called surface waves for radio waves and thus are the origin for surface plasmons polaritons.

Later, Gustav Mie gave the theoretical description for scattering of light on very small spherical particle and gave the outline description of localized plasmons resonance.

## Theoretical description on Plasmonics

### Drude Model

In 1900, Paul Drude a German scientist gave the theory in which the conduction of metal i.e thermally or electrically by applying the kinetic theory of gases and can be considered as electron gas [25] [26]. he assume that conduction electron in the metal is like a molecules in the gas theory and he suggested that the positive ions are immobile and electrons are moving in the metals and electrons are scattered on both side i.e. with other electrons and positive base.

This mechanism is shown in figure 3.1.

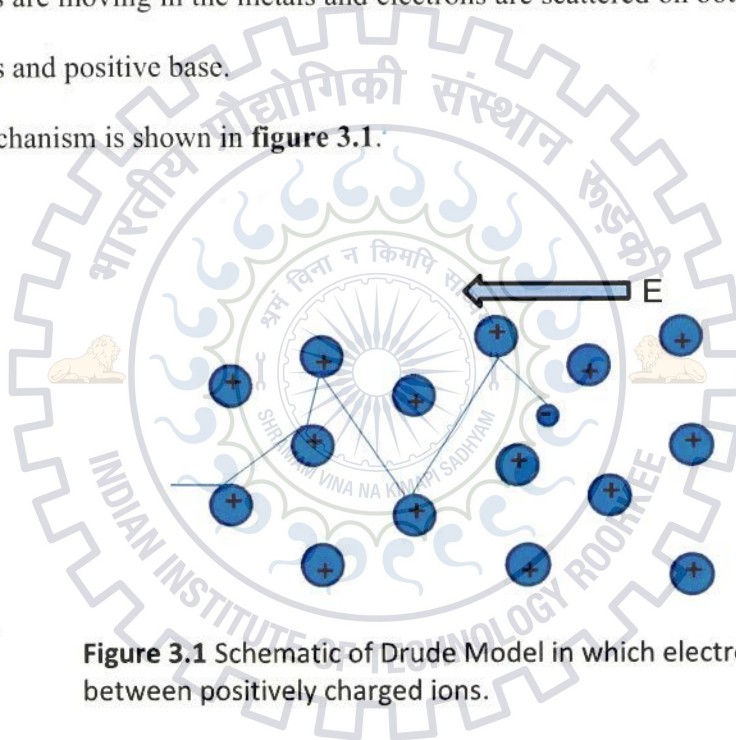


**Figure 3.1** Schematic of Drude Model in which electrons are collided between positively charged ions.

According to this model free electron gas is represented as:

$$\varepsilon(\omega) = 1 - \frac{ne^2}{\varepsilon_0 m \omega^2} \quad (3.1)$$

Where  $\epsilon_0$  =vacuum permittivity

$n$ =electron density

$m$  and  $e$  are the mass and electron charge

And the plasma frequency with equal positive and negative charge in a medium can be represented as:

$$\omega_p^2 = \frac{ne^2}{\epsilon_0 m} \quad (3.2)$$

From equation 3.1 & 3.2, dielectric function is given by

$$\epsilon(\omega) = 1 - \frac{\omega_p^2}{\omega^2} \quad (3.3)$$

If  $\epsilon_\infty$  is the constant offset, this added the interband transition effect above plasma frequency, then the dielectric function can be represented as

$$\epsilon(\omega) = \epsilon_\infty - \frac{\omega_p^2}{\omega^2} \quad (3.4)$$

## Plasmons

The oscillation of free electron density in opposite to background of positive ions in metal constitutes Plasmons. This oscillation is longitudinal in nature caused by Coulomb force and originates from long range correlation of the electrons. The quantization of oscillation of plasma just as phonons and photons are mechanical vibration and quantization of light respectively resulting as quasiparticles. Thus collective oscillations of the free electron gas density are plasmons, for example, at optical frequencies. Coupling of the plasma with a photon to create another quasiparticle called plasma polariton.

To imagine this incident a metal slab (rectangular) which is sited in an external electric field (shows as left). Positive ions moves to the left and electrons will moves in the right (from **figure 3.2**). The movement of electrons is continuous until the field inside the metal will cancel. The electrons will repel by each other and attracted towards positive ions on the left side. The movement of electrons is back and forth at the frequency and it is represented by expression 3.2

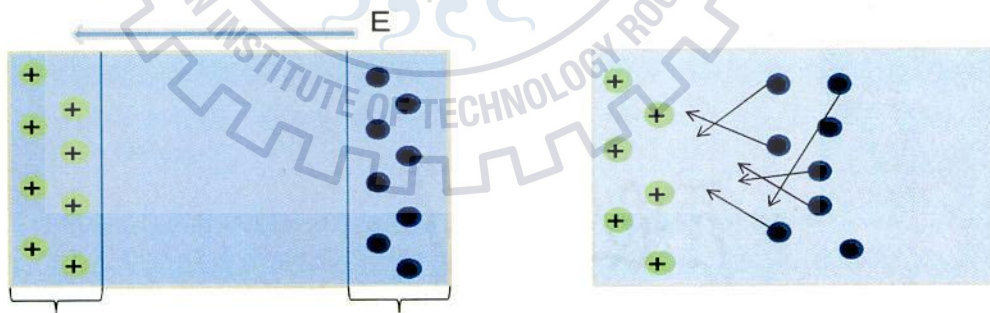


**Figure 3.2** Simple diagram of plasma oscillation (a) due to external electric field charges are separated. (b) Without electric field electrons moves back.

Theoretically and experimentally these oscillation of plasma in gaseous discharge is described by Langmuir [27]. Within a metal the oscillation of plasma with a frequency by drude model (Eq 3.2) are known as bulk plasmons.

With the complexity of dielectric function (Eq 3.4), damping coefficient can be represented as:

$$\varepsilon(\omega) = \omega^2 - \frac{\omega_p^2}{\omega^2 + iY\omega} \quad (3.5)$$

Where  $Y$  = damping term

The real and imaginary part of  $\varepsilon(\omega)$  can be represented as:

$$\varepsilon'(\omega) = \varepsilon_{\infty} - \frac{\omega_p^2}{\omega^2 + Y^2} \quad (3.6)$$

$$\varepsilon''(\omega) = \frac{\omega_p^2 Y}{\omega(\omega^2 + Y^2)} \quad (3.7)$$

Because of the oscillation of electrons i.e. out of phase with the electric field vector of the light wave, from (Eq 3.6) it can be deduce that below the whole frequency of bulk plasmons of a metal i.e.  $\varepsilon' < 0$

From  $\varepsilon'(\omega) = 0$ , this represent that the frequency of the longitudinal modes of oscillation therefore the longitudinal plasma frequency can be represented as:

$$\omega_p^2 = \omega^2 + Y^2 \quad (3.8)$$

The oscillation occurs until the energy is nowhere found due to damping .these oscillation are known as plasma.

In the optical properties of metals, the plasma plays a huge role. Incoming light radiation of frequency below the plasma frequency is reflected because in the metals the electrons screen the electric field of the light and the light radiation of frequency above the plasma frequency is transmitted, because electrons in the metals cannot respond faster. In some metals for example gold and copper, in the visible region have electronic interband transition and absorption of specific colors occurs. The materials properties of metals reflect in the bulk plasmons. But this phenomenon cannot carry the surface information; due to this another term has evolved in which there are surface contribution i.e. surface plasmons.

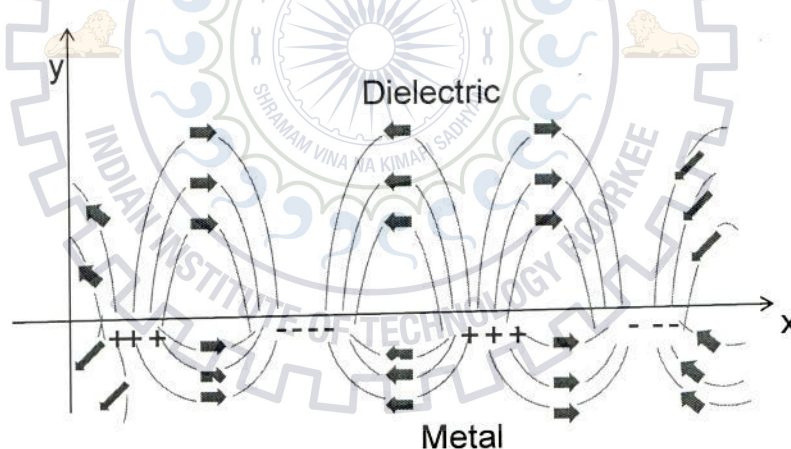


Figure 3.3. Representation of a propagation of surface plasmon along a metal-dielectric interface

Surface plasmons are the electromagnetic waves that propagate along the interface of a metal-dielectric junction. It is generated in the form of a collective oscillation of

## Surface Plasmons

By solving the Maxwell equation that gives a surface bound mode between the metal & dielectric interface. Or we can say that the coherent electron oscillations that exist between any two media constitutes the surface Plasmon's in which the sign of the real part of the dielectric function of the materials changes across the interface (e.g. metal-dielectric interface, such as metal sheet in air). In this, the oscillation of the free electrons responds collectively in resonance with the light wave [28] [29]. The energy of the surface plasmons is lower than the bulk plasmons. The resulting hybridized excitation when surface plasmons couple with the photons known as surface plasmons polaritons (SPP). The direction of the surface plasmons polariton is along the surface of the metal until the energy is lost either by radiation into the free space or absorption in the metal.



**Figure 3.3.** Representation of a propagation of electron density wave along a metal-dielectric interface.

Surface plasmons are the electromagnetic waves that parallelly propagate along the metal-dielectric interface. It is quantized oscillation (i.e. collectively) of the conduction

electrons along the surface of the semiconductors or metals. In the view of the facts that the wave on the boundary of the external medium and the metal (for example air and water) these are very sensitive oscillation to any change of this boundary such as the absorption at the metal surface. The generation of surface plasmons are within a continuous thin film (within the range of 30-50nm) by using arrangement of in which when light is incident on the film from a medium of greater than 1 index of refraction.

Surface plasmons are excited by the photons incident at the interface of metal and air and can decay back into photons as confirmation by the increased radiation intensity of light from the film as decreases reflected intensity.





## The wave equation

For observing physical properties of surface plasmons we apply Maxwell equation to the conductor and dielectric interface we get

$$\nabla \cdot D = \rho_{ext} \quad (3.9)$$

$$\nabla \cdot B = 0 \quad (3.10)$$

$$\nabla \times E = -\frac{\partial B}{\partial t} \quad (3.11)$$

$$\nabla \times H = J_{ext} + \frac{\partial D}{\partial t} \quad (3.12)$$

In the absence of current densities and external charge. The equations (3.11) and (3.12) can be represented as:

$$\nabla \times \nabla \times E = -\mu_0 \frac{\partial^2 D}{\partial t^2} \quad (3.13)$$

Using equations  $\nabla \times \nabla \times E = \nabla(\nabla \cdot E) - \nabla^2 E$  as well as  $\nabla \cdot (\epsilon E) = E \cdot \nabla \epsilon + \epsilon \nabla \cdot E$  and remembering that, due to the absence of external simulation  $\nabla \cdot D = 0$  (Eq 3.17) can be rewritten as

$$\nabla \left( -\frac{1}{\epsilon} E \cdot \nabla \epsilon \right) = \nabla^2 E = \mu_0 \epsilon_0 \epsilon \frac{\partial^2 E}{\partial t^2} \quad (3.14)$$

If we assume that the dielectric profile  $\epsilon = \epsilon(r)$  over the distances on the order of one optical wavelength is negligible (Eq 3.14) of the electromagnetic wave theory is written as

$$\nabla^2 E - \frac{\epsilon}{c^2} \frac{\partial^2 E}{\partial t^2} = 0 \quad (3.15)$$

We solve (Eq 3.15) separately in the region of constant ( $\epsilon$ ) and matched the obtained solutions using appropriate boundary conditions to cast (Eq 3.15) in a form suitable for the description of confined propagation waves, for this we precede into two steps. First, we assume that a harmonic time dependence  $E(r, t) = E(r) \exp^{-i\omega t}$  of the electric field this is inserted into (Eq 3.15) that represented as:

$$\nabla^2 E + k_0^2 \epsilon E = 0 \quad (3.16)$$

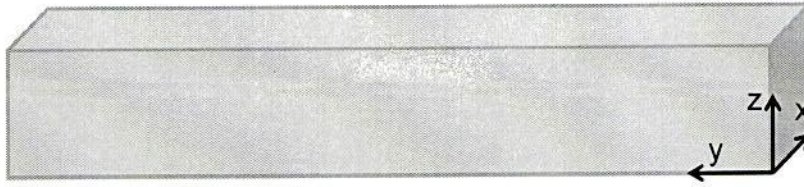


**Figure 3.4** Geometry of the planar waveguide.

Where  $k_0 = \omega/c$  is the wave vector of the propagating wave in vacuum (Eq 3.16) is called as **Helmholtz equation**. We assume a one-dimensional problem to define the propagation geometry. The Cartesian coordinate system propagates along the X-direction and no spatial variation shows perpendicularly in the y-direction plane figure (3.4). Therefore  $\epsilon = \epsilon(z)$ . When this is applied to the problem of electromagnetic surface, the plane  $z=0$  coincides with the propagating wave interface can be written as  $E(x, y, z) = E(z)e^{i\beta x}$  and the complex parameter  $\beta = k_x$  is called as the propagation constant that corresponds to the component of the wave vector of the travelling waves in the propagation direction. Inserting this into (Eq 3.16) yields the desired form of the wave equation

$$\frac{\partial^2 E(z)}{\partial z^2} + (k_0^2 \epsilon - \beta^2)E = 0$$

(3.17)

The same equation occurs for the magnetic field H. From (Eq 3.17) we know the general description of the guided electromagnetic modes in waveguides. For determining the dispersion of propagating wave and spatial profile, we now need to find explicit expression for different component i.e. electric field and magnetic field. This can be achieved by using the curl equations (3.11) (3.12)

For Harmonic time dependence  $\frac{\partial}{\partial t} = -i\omega$  we arrive at the following set of coupled equations.

$$\frac{\partial E_z}{\partial y} - \frac{\partial E_y}{\partial z} = i\omega\mu_0 H_x \quad (3.18)$$

$$\frac{\partial E_x}{\partial z} - \frac{\partial E_z}{\partial x} = i\omega\mu_0 H_y \quad (3.19)$$

$$\frac{\partial E_y}{\partial x} - \frac{\partial E_x}{\partial y} = i\omega\mu_0 H_z \quad (3.20)$$

$$\frac{\partial H_z}{\partial y} - \frac{\partial H_y}{\partial z} = i\omega\epsilon_0\epsilon E_x \quad (3.21)$$

$$\frac{\partial H_x}{\partial z} - \frac{\partial H_z}{\partial x} = i\omega\epsilon_0\epsilon E_y \quad (3.22)$$

$$\frac{\partial H_y}{\partial x} - \frac{\partial H_x}{\partial y} = i\omega\epsilon_0\epsilon E_z \quad (3.23)$$

For x-direction propagation  $\frac{\partial}{\partial x} = i\beta$  and homogeneity in the y-direction  $\frac{\partial}{\partial y} = 0$  this equation simplifies and represented as:

$$\frac{\partial E_y}{\partial z} = -i\omega\mu_0 H_z \quad (3.24)$$

$$\frac{\partial E_x}{\partial z} - i\beta E_z = i\omega\mu_0 H_y \quad (3.25)$$

$$i\beta E_y = i\omega\mu_0 H_z \quad (3.26)$$

$$\frac{\partial H_y}{\partial z} = i\omega\varepsilon_0 \varepsilon E_x \quad (3.27)$$

$$\frac{\partial H_z}{\partial x} - i\beta H_z = -i\omega\varepsilon_0 \varepsilon E_y \quad (3.28)$$

$$i\beta H_y = -i\omega\varepsilon_0 \varepsilon E_y \quad (3.29)$$

From this, two set of self consistent solutions occurs with polarization properties of the propagating waves. In the former there are transverse magnetic (TM) modes, in this the field component  $E_x$ ,  $E_y$  and  $H_y$  are non zero, and in the later there are transverse electric (TE) modes with  $H_x$ ,  $H_y$  and  $E_y$  are nonzero. for TM modes (Eq 3.24 to 3.29) deduce to

Surface Plasmon at Metal-Dielectric Interface

$$E_x = -i \frac{1}{\omega \epsilon_0 \epsilon} \frac{\partial H_y}{\partial z}$$

TM Mode

(3.30)

The easy way to understand the picture of the surface plasmons at the single interface (figure 3.4) between a non absorbing half space ( $z > 0$ ) a dielectric with an adjacent conducting half space ( $z < 0$ ) and positive real dielectric constant  $\epsilon$ . This is due to the necessity of metallic character infer that  $\epsilon$  is at frequency below the bulk frequency  $\omega_p$ , this condition is satisfied by surface propagating wave solutions in the  $z$  direction perpendicular to the interface.

$$E_x = -i \frac{\beta}{\omega \epsilon_0 \epsilon} H_y$$

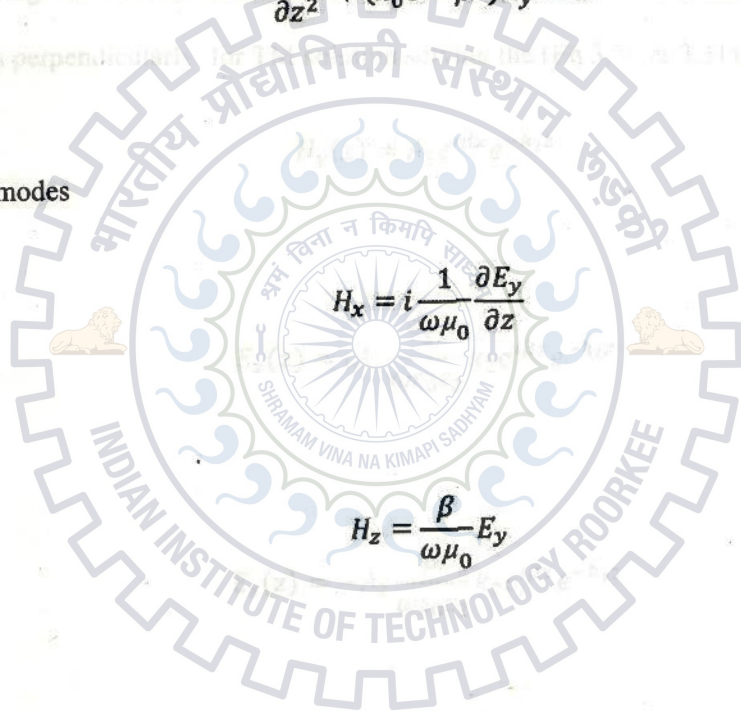
(3.31)

Wave equation for TM modes is

$$\frac{\partial^2 H_y}{\partial z^2} + (k_0^2 \epsilon - \beta^2) H_y = 0$$

(3.32)

For TE modes



$$H_x = i \frac{1}{\omega \mu_0} \frac{\partial E_y}{\partial z}$$

(3.33)

$$H_z = \frac{\beta}{\omega \mu_0} E_y$$

(3.34)

Wave equation for TE modes is

$$\frac{\partial^2 E_y}{\partial z^2} + (k_0^2 \epsilon - \beta^2) E_y = 0$$

(3.35)

This all constitutes the detailed description of surface plasmons.

## Surface Plasmon at Metal Dielectric interface

### TM Mode

The easy way to understand the picture of the surface plasmons at the single interface (figure 3.4) between a non absorbing half space ( $z>0$ ) a dielectric with an adjacent conducting half space ( $z<0$ ) and positive real dielectric constant  $\epsilon_0$ . This is described from the dielectric function  $\epsilon_1(\omega)$ . The necessity of metallic character infer that  $\text{Re}[\epsilon_1]<0$ , at frequency below the bulk frequency  $\omega_p$ , this condition is satisfied for metals for propagating wave solutions this is confined to the interface with evanescent decay in  $z$ -direction perpendicularly, for TM solution solving the (Eq 3.30 & 3.31) that yields as:

$$H_y(z) = A_2 e^{i\beta x} e^{-k_2 z} \quad (3.36)$$

$$E_x(z) = iA_2 \frac{1}{\omega \epsilon_0 \epsilon_2} k_2 e^{i\beta x} e^{-k_2 z} \quad (3.37)$$

$$E_z(z) = -A_2 \frac{\beta}{\omega \epsilon_0 \epsilon_2} k_2 e^{i\beta x} e^{-k_2 z} \quad (3.38)$$

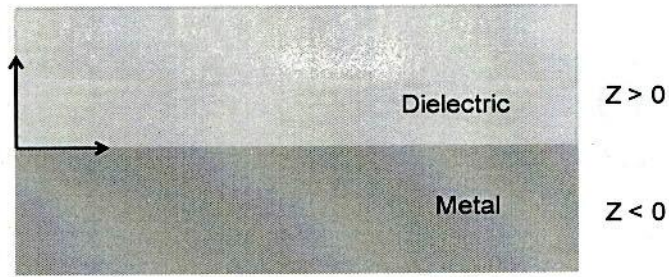


**Figure 3.5** schematic of geometry for SPP propagation between metal dielectric interfaces.

For  $z < 0$

$$H_y(z) = A_1 e^{i\beta x} e^{-k_1 z} \quad (3.39)$$

$$E_x(z) = -iA_1 \frac{1}{\omega \epsilon_0 \epsilon_1} k_1 e^{i\beta x} e^{-k_1 z} \quad (3.40)$$

$$E_z(z) = -A_1 \frac{\beta}{\omega \epsilon_0 \epsilon_1} k_1 e^{i\beta x} e^{-k_1 z} \quad (3.41)$$

$k_i = k_{z,i}$  ( $i = 1, 2$ ) in the interface of the two media, this is the perpendicular component of the wave vector. If we reciprocal it  $\tilde{z} = 1/|k_z|$  the field is perpendicular to the surface that represent the evanescent decay length.

If  $A_1 = A_2$  this is the requirement of continuity of the  $H_y$  &  $\epsilon_i E_z$



$$\frac{k_2}{k_1} = -\frac{\epsilon_2}{\epsilon_1}$$

(3.42)

Confinement to the surface demands  $R_c[\epsilon_1] < 0$  if  $\epsilon_2 > 0$  between a conductor and insulator, the surface wave occurs at the interface, therefore  $H_y$ , the wave equation (Eq 3.32) can be represented as:

$$k_1^2 = \beta^2 - k_0^2 \epsilon_1$$

(3.43)

$$k_2^2 = \beta^2 - k_0^2 \epsilon_2$$

(3.44)

Combining (Eq 3.42) with (3.43 & 3.44) we get

$$\frac{k_2^2}{k_1^2} = \frac{\beta^2 - k_0^2 \epsilon_2}{\beta^2 - k_0^2 \epsilon_1}$$

(3.45)

From equation (3.42) & (3.45) we get,

$$\frac{\epsilon_2^2}{\epsilon_1^2} = \frac{\beta^2 - k_0^2 \epsilon_2}{\beta^2 - k_0^2 \epsilon_1}$$

(3.46)

$$\beta^2 = k_0^2 \left( \frac{\epsilon_1 \epsilon_2^2 - \epsilon_2 \epsilon_1^2}{\epsilon_2^2 - \epsilon_1^2} \right)$$

(3.47)

$$\beta^2 = k_0^2 \left( \frac{\epsilon_1 \epsilon_2 (\epsilon_2 - \epsilon_1)}{(\epsilon_2 - \epsilon_1)(\epsilon_1 + \epsilon_2)} \right)$$

(3.48)

So now we get dispersion relation of surface plasmons propagating between two half space interfaces

$$\beta = k_0 \sqrt{\left( \frac{\epsilon_1 \epsilon_2}{\epsilon_1 + \epsilon_2} \right)}$$

(3.50)

This is valid for real and complex  $\epsilon_1$ , i.e. for conductor without or with attenuation

**TE mode**

Using (Eq 3.32 to 3.35) the field component expression can be represented as

$$E_y(z) = A_2 e^{i\beta x} e^{-k_2 z}$$

(3.51)

$$H_x(z) = -iA_2 \frac{1}{\omega \mu_0} k_2 e^{i\beta x} e^{-k_2 z}$$

(3.52)

$$H_z(z) = A_2 \frac{\beta}{\omega \mu_0} e^{i\beta x} e^{-k_2 z}$$

(3.53)

For  $z > 0$

$$E_y(z) = A_1 e^{i\beta x} e^{-k_2 z} \quad (3.54)$$

$$H_x(z) = -iA_1 \frac{1}{\omega \mu_0} k_1 e^{i\beta x} e^{-k_2 z} \quad (3.55)$$

$$H_z(z) = A_1 \frac{\beta}{\omega \mu_0} e^{i\beta x} e^{-k_1 z} \quad (3.56)$$

For  $z < 0$  at the interface, the continuity of  $E_y$  &  $H_x$  leads to the condition

$$A_1(k_1 + k_2) = 0 \quad (3.57)$$

For  $\text{Re}[k_1] > 0$  &  $\text{Re}[k_2] > 0$  this is fulfilled only if  $A_1 = 0$ , and also  $A_2 = A_1 = 0$ . In TE polarization no surface modes exists. So in TM polarization surface plasmons exists.

## Surface Plasmons Excitation

Electrons are responsible for excitation of surface Plasmon, but experimentally it is more easily realized by the excitation of surface plasmons through light. Firstly In this light is p-polarized. However to excite surface plasmons it needed a specific methods for coupling with light radiation. Since plasmons has a greater wave vector as compared with wave vector of light for the same energies. This means that the dispersion curve of the surface plasmons  $\omega(k)$  occurs at the right side of the dispersion curve and can be represented as

$$\frac{\omega}{c} \sqrt{\epsilon} < \frac{\omega}{c_0} \sqrt{\frac{\epsilon_1 \epsilon_2}{\epsilon_1 + \epsilon_2}}$$

(3.58)



$$k_{ph} < k_{sp}$$

(3.59)

Where  $k_{sp}$  = wave vector of plasmons

$k_{ph}$  = wave vector of the phonons

Since, the wave vectors of the surface plasmons and the incident electromagnetic radiation do not match because the dispersion curves do not intersects each other, that's why surface plasmons are non-radiative and cannot propagate into empty spaces. But the magnitude of the wave vector  $k$  of the incident light radiation on the air-metal boundary increases for a given frequency  $\omega$ , then intersects of the dispersion curve takes place.

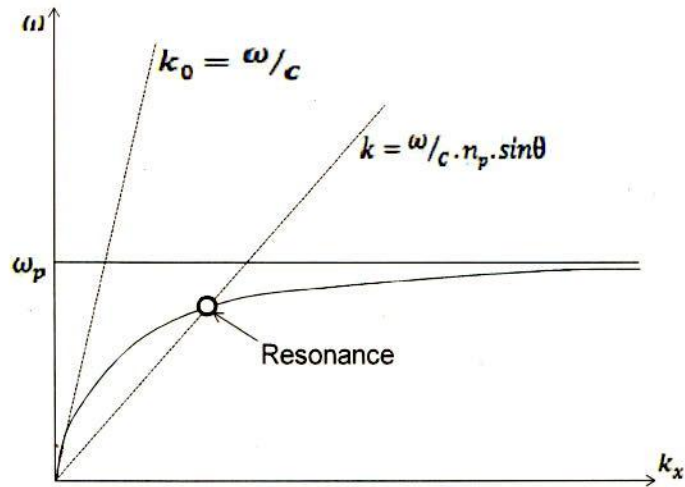


**Figure 3.6** Dispersion curves for surface plasmons.

Physically this can be executed when the incident light radiation passes through a medium like glass or on which metal film is deposited. The glass has a tendency of multiplying the wave number by  $n_p$  (index of refraction of glass). From **figure 3.6** with the proper thickness of the metal film some of the incident light radiation is transmitted through the metal-air boundary in which the surface plasmons are excited through grating coupling the wave vector can also be increased.

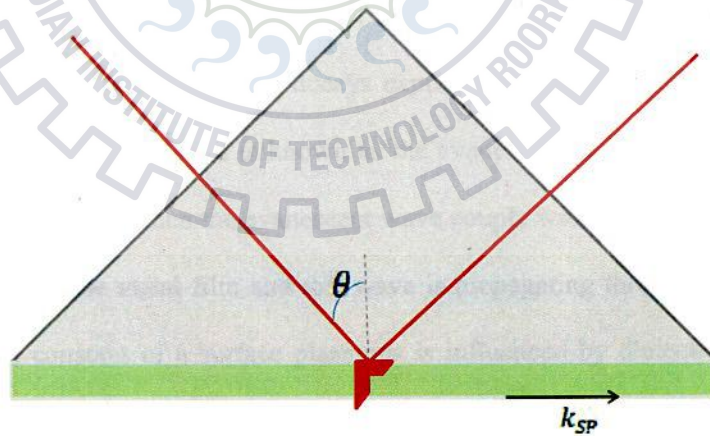


**Figure 3.7** Kretschmann Configuration for attenuated total reflection method

## Prism coupling

The attenuated total reflection method (ATR) is used to excite surface plasmons this is very common method. This method employs the evanescent wave conception of TIR (Total Internal Reflection). To measure the fluctuation that happens when a total internally reflected light radiation beams interacts with a sample. There are two possible ways of ATR.

- (i) Kretschmann configuration
- (ii) The Otto configuration

In the kretschmann configuration, a prism of high refractive index ( $n_p$ ) is directly in contact with the thin metal film with thickness  $q$  and permittivity  $\epsilon_m$  and refractive index  $n_d$  ( $n_d < n_p$ ) and metal film have a semi infinite dielectric medium see **figure 3.7**

When the radiated light wave is propagates in the prism and then propagates to the metal film as a result a part of the light wave is propagating in the metal film as an electromagnetic wave [30] & rest of the light wave is reflected back from the prism and the propagating electromagnetic wave decays exponentially in perpendicular directions to the prism-metal interface. This is known as the evanescent wave ,if the thickness of the metal film is very thin then the evanescent wave couple with the surface plasmons at the outer surface of the metal film and this wave is propagating through the metal film .the propagation constant of a surface plasmons is influenced by dielectric medium on the outer side of the metal film and that is propagating along the thin film this can be represented as

$$\beta^{sp} = \beta_0^{sp} + \Delta\beta = \frac{\omega}{c} \sqrt{\frac{\epsilon_d \epsilon_m}{\epsilon_d + \epsilon_m}} + \Delta\beta$$

(3.60)

Where  $\beta_0^{sp}$  propagation constant of the surface plasmons that is propagating at the interface of the metal dielectric in absence of the prism.  $\Delta\beta$  Represented the finite metal film thickness in the presence of the prism. For coupling, the evanescent wave propagation constant is equal to that of the surface plasmons which can be represented as

$$\beta^{EW} = Re\{\beta^{SP}\}$$

(3.60)



$$\frac{2\pi}{\lambda} n_p \sin\theta = Re\left\{\frac{\omega}{c} \sqrt{\frac{\epsilon_d \epsilon_m}{\epsilon_d + \epsilon_m} + \Delta\beta}\right\}$$

(3.61)

In terms of effective index,

$$n_{ef}^{EW} = Re\{n_{ef}^{SP}\}$$

(3.62)



$$n_p \sin\theta = Re\left\{\frac{\omega}{c} \sqrt{\frac{\epsilon_d \epsilon_m}{\epsilon_d + \epsilon_m} + \Delta n_{ef}^{SP}}\right\}$$

(3.63)

Where  $n_{ef}^{EW}$  represents the effective index of the evanescent wave,

$\Delta n_{ef}^{SP}$  Represents the perturbation term,

$n_{ef}^{SP}$  is the surface plasmons effective index.

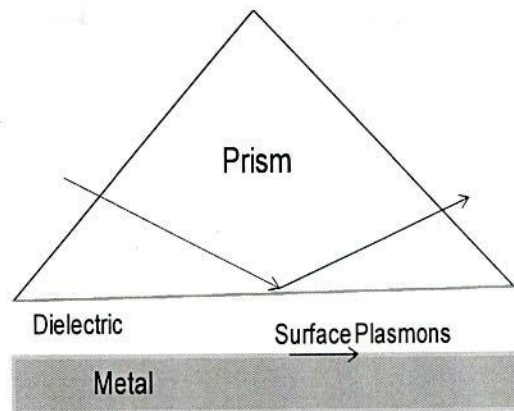


**Figure 3.8** Otto configurations for surface plasmons coupling.

In Otto configuration **figure 3.8** the prism of high refractive index consisting of a thin dielectric film is interfaced with a metal dielectric waveguide in which the refractive index of dielectric is smaller to that of prism and thickness is  $q$ .

In this, the light wave is incident with an angle greater than the critical angle on the prism-dielectric interface; it can produce an evanescent wave between the interface of dielectric film and prism. If appropriate thickness is taken the coupling of the surface plasmons with the evanescent wave occurs at interface of metal-dielectric and the propagation constants of the surface plasmons and evanescent wave are equal.



# **CHAPTER 4**

## ***PLASMONICS PROPERTIES OF PULSED LASER DEPOSITED METAL THIN FILM***



## Optical Properties

Silver films of different thickness are deposited on glass substrates using pulsed laser deposition technique (PLD) and the glass substrates are then pasted on the hypotenuse face of the prism by Canada balsam paste. 2 days require to dry Canada balsam adhesive for fixing the silver deposited glass substrates on prism. Index of refraction at  $\lambda=632.8\text{nm}$  of BK 7 is  $n=1.5150$ . Surface plasmons can be observed by rotating the prism on the rotation table by measuring the reflectance as a function of angle of incidence. Unpolarized He-Ne laser is passed through the polarizer to get p-polarized beam that is incident on the prism air interface at an incident angle  $\theta$  above critical angle. The reflected laser beam could be monitored even on the white paper by naked eyes. Incident intensity is approximately equal to the reflected intensity at the critical angle for total internal reflection. Reflectivity of the curve was first observed to decrease sharply and then increase again. At the resonance angle surface plasmons are excited where the reflection dip is occurred. It is expected that where no surface plasmons are excited the reflectivity is equal to unity and due to the loss of energy of the attenuated total reflection generated evanescent field in the metal the reflectivity is never equal to unity. Photo detector which is connected to a power meter is used to observe the intensity drop as a function of angle of incidence after reflecting from the metal-air interface through the prism.

### Measured incidence angle dependence

*For Red light of wavelength  $\lambda=6328 \text{ \AA}$*

The surface plasmons excitation was examined in silver metal-air interface and a reflected intensity dip was observed at an incident angle  $43.67^\circ$  for 6000,  $45^\circ$  for 7000,  $46.32^\circ$  for 8000 and  $46.98^\circ$  for 9000 number of laser pulses as shown in **Figure 4.1** and

at an incident angle  $45.33^\circ$  for 10000,  $41.36^\circ$  for 12000,  $41.03^\circ$  for 14000 number of laser pulses as shown in **figure 4.2**. **Figure 4.3 - 4.9** shows the comparison of experimental and theoretical results for 6000, 7000, 8000, 9000 number of laser pulses.

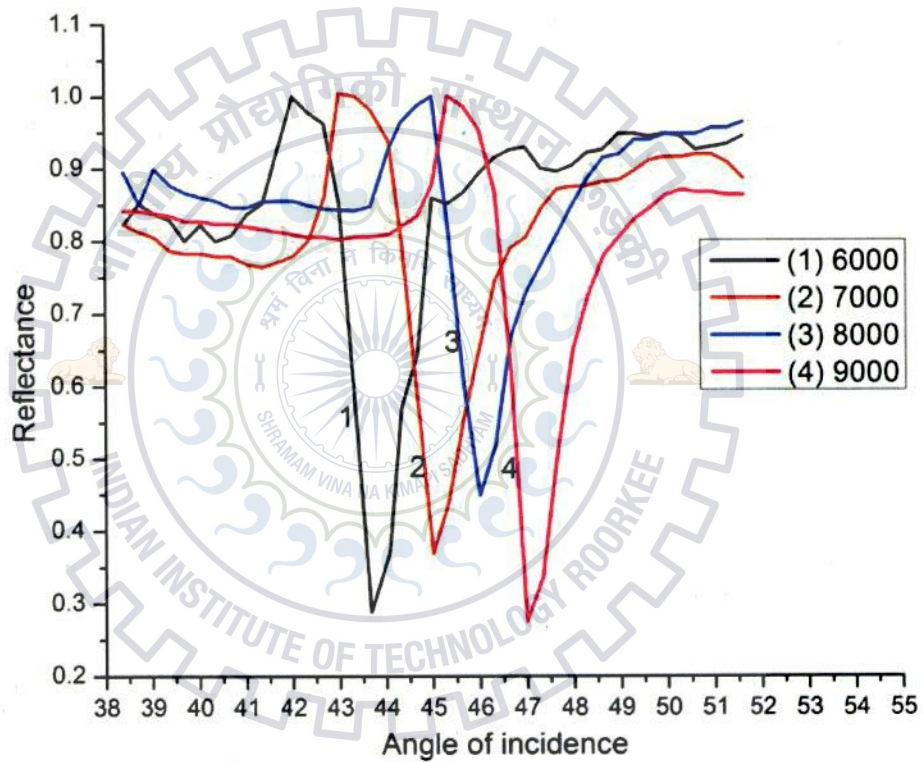


**Figure 4.1** Reflectivity Vs angle of incidence SPR curves of 6000, 7000, 8000, 9000 number of pulses silver films.

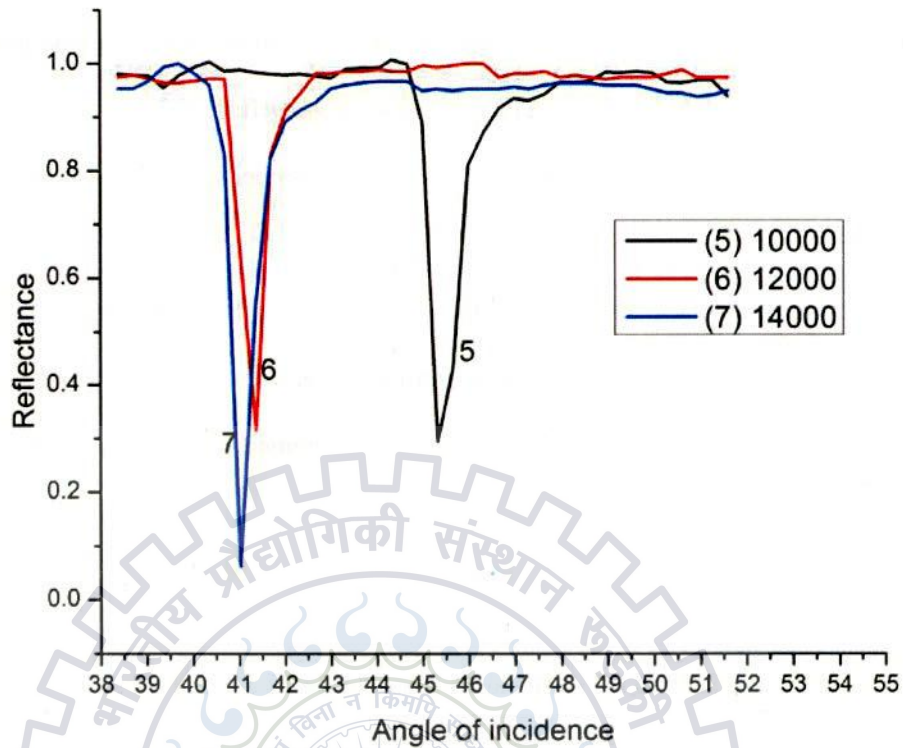


**Figure 4.2** Reflectivity Vs angle of incidence SPR curves of 10000, 12000, 14000 number of pulses silver films.

From **Figure 4.1 & 4.2** the measured SPR curves is shown and the obtained SPR reflectance curve for Ag-air mode was simulated theoretically by using Fresnel relations  $\epsilon_2=1$  for air. **Figures 4.3-4.9** shows a arrangement between the experimental and theoretical curve and data as shown in **Table 2**, The SPR dip angle depends on the real part of the dielectric constant of the silver film, whereas the imaginary part of the dielectric constant and thickness of the metal film influence the width and reflectance dip of the SPR reflectance curve.

From theoretical simulation using a non commercial software Matlab code Winspal 302 we analyse that as the real part of dielectric constant of metal films increases the SPR dip angle also increases up to 9000 number of pulses and then SPR dip angle is decreases as

the real part of dielectric constant decreases in 10000, 12000 & 14000 number of pulses films as shown in **Figures 4.3-4.9**.

As the imaginary part of dielectric constant and the metal thickness depends on the width and dip reflectance of SPR reflectance curve from **Figures 4.1 & 4.2** it can be seen that as the thickness of the film increases width of the SPR reflectance curve[35] becomes narrower.

Thickness of metal layer is one of the main parameters of SPR. Metal film must be thin enough that the evanescent wave is able to penetrate through the metal film and excite surface plasmons in the outer boundary of metal film. On the other hand, it must be thick enough that evanescent wave cannot excite the free electrons out of the surface [36], which results lower quality of SPR phenomenon.

**Table 2**

Number of pulses	Dielectric constants of silver films	Thickness(nm)
6000	-10.7+0.327i	51.2
7000	-7.99+0.135i	64.2
8000	-6.92+0.099i	67.6
9000	-6.12+0.131i	73.1
10000	-7.50+0.094i	78
12000	-21.42+0.10i	80
14000	-25.4+0.013i	88.2

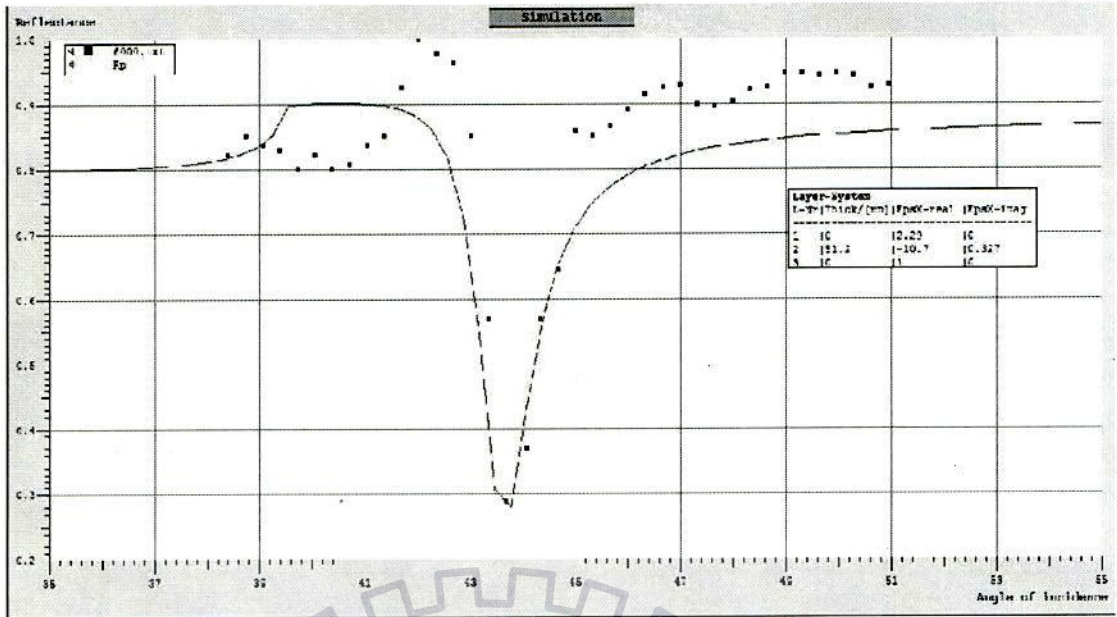


Figure 4.3 Comparison between experimental and theoretical results for 6000 number of pulses film.

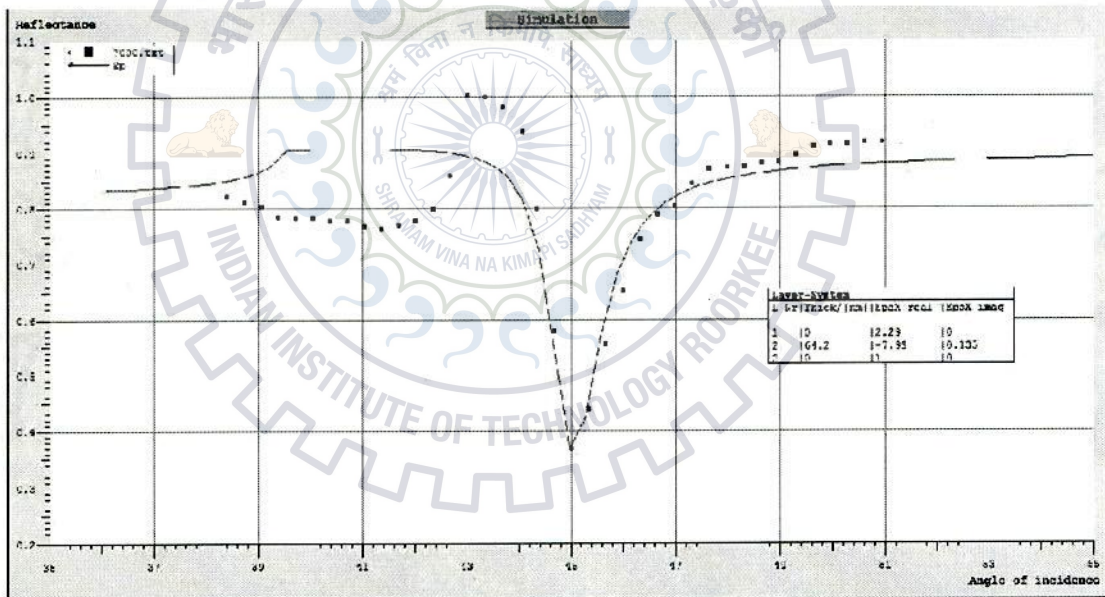


Figure 4.4 Comparison between experimental and theoretical results for 7000 number of pulses film.

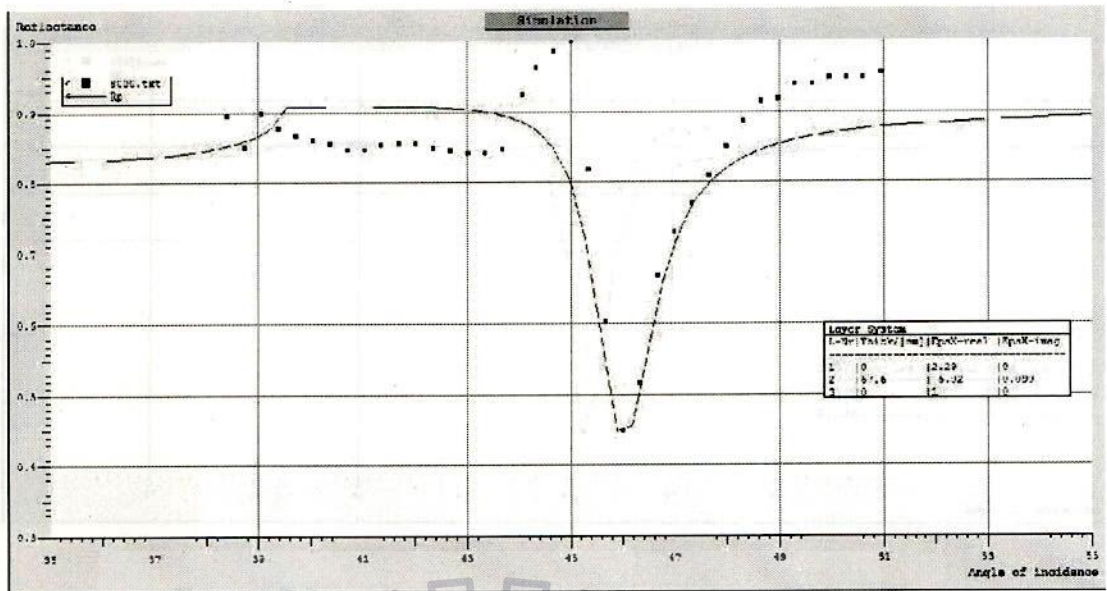


Figure 4.5 Comparison between experimental and theoretical results for 8000 number of pulses film.

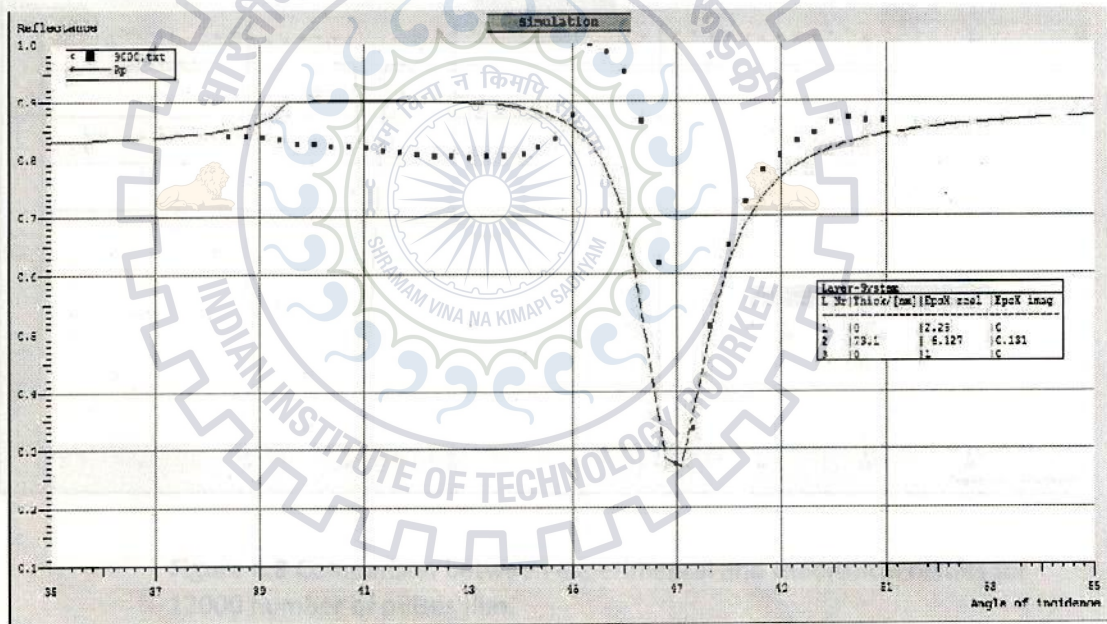


Figure 4.6 Comparison between experimental and theoretical results for 9000 number of pulses film.

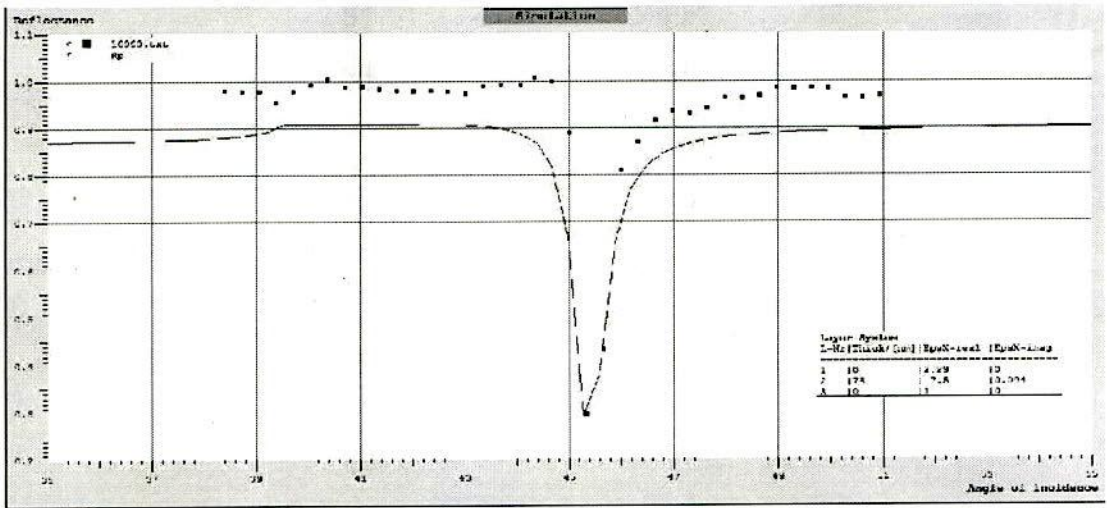


Figure 4.7 Comparison between experimental and theoretical results for 10000 number of pulses film.

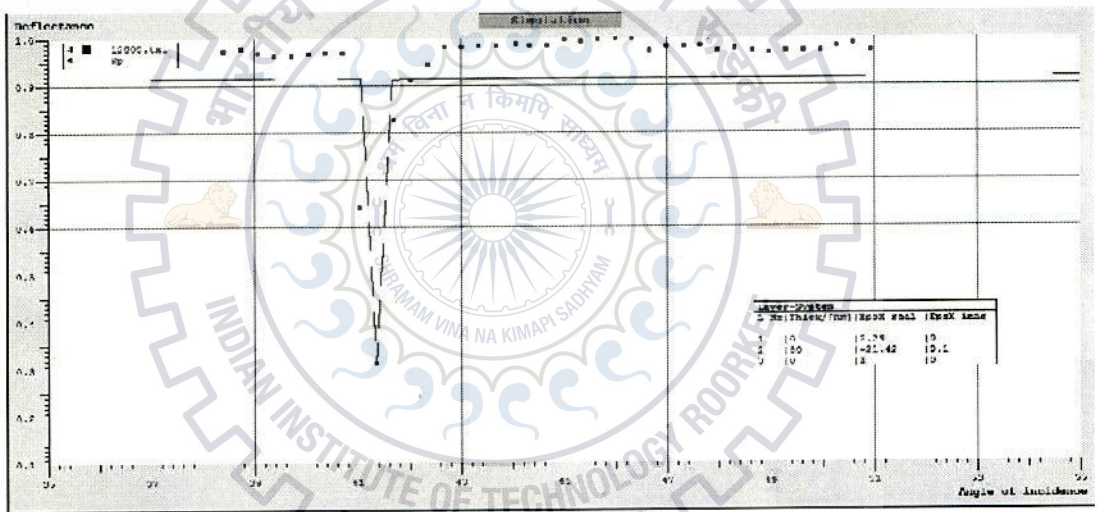


Figure 4.8 Comparison between experimental and theoretical results for 12000 number of pulses film.



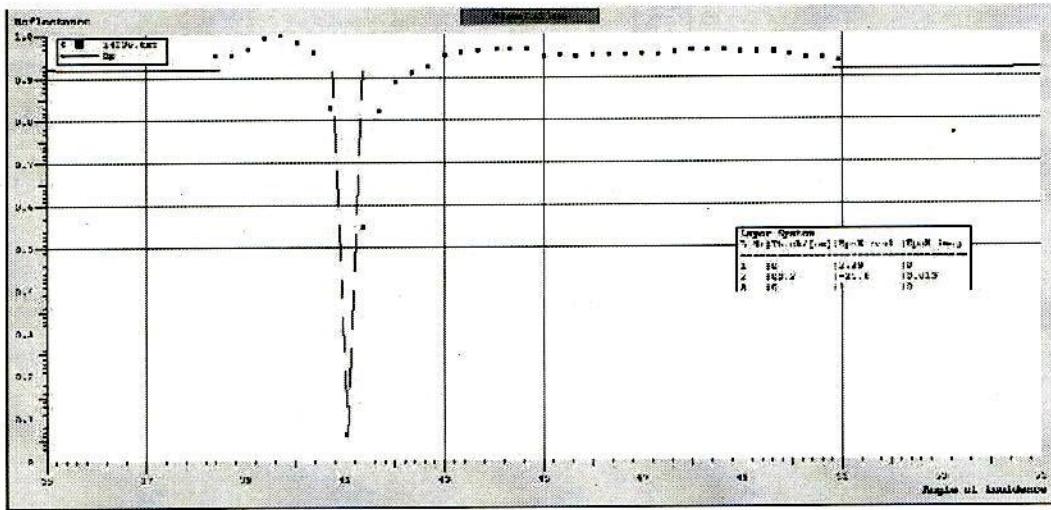
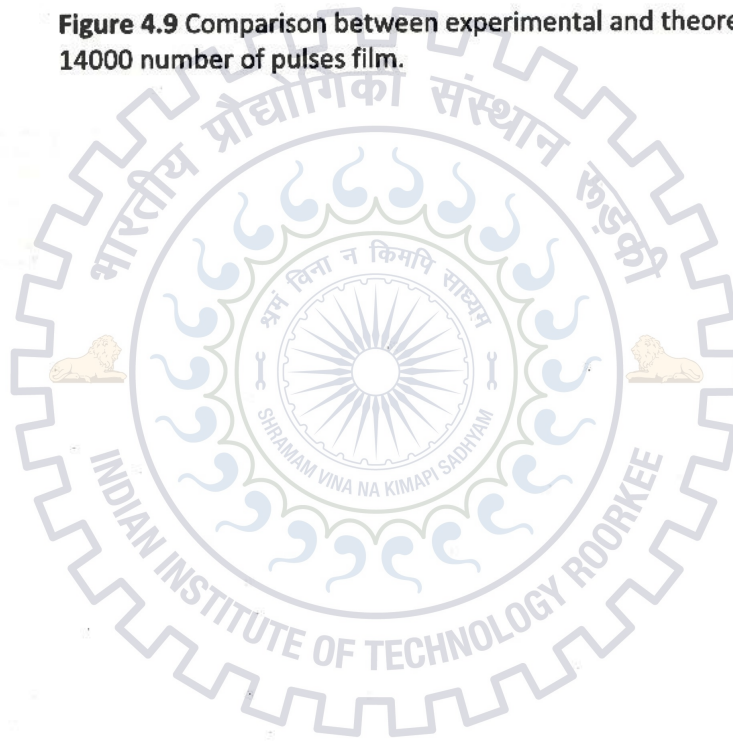
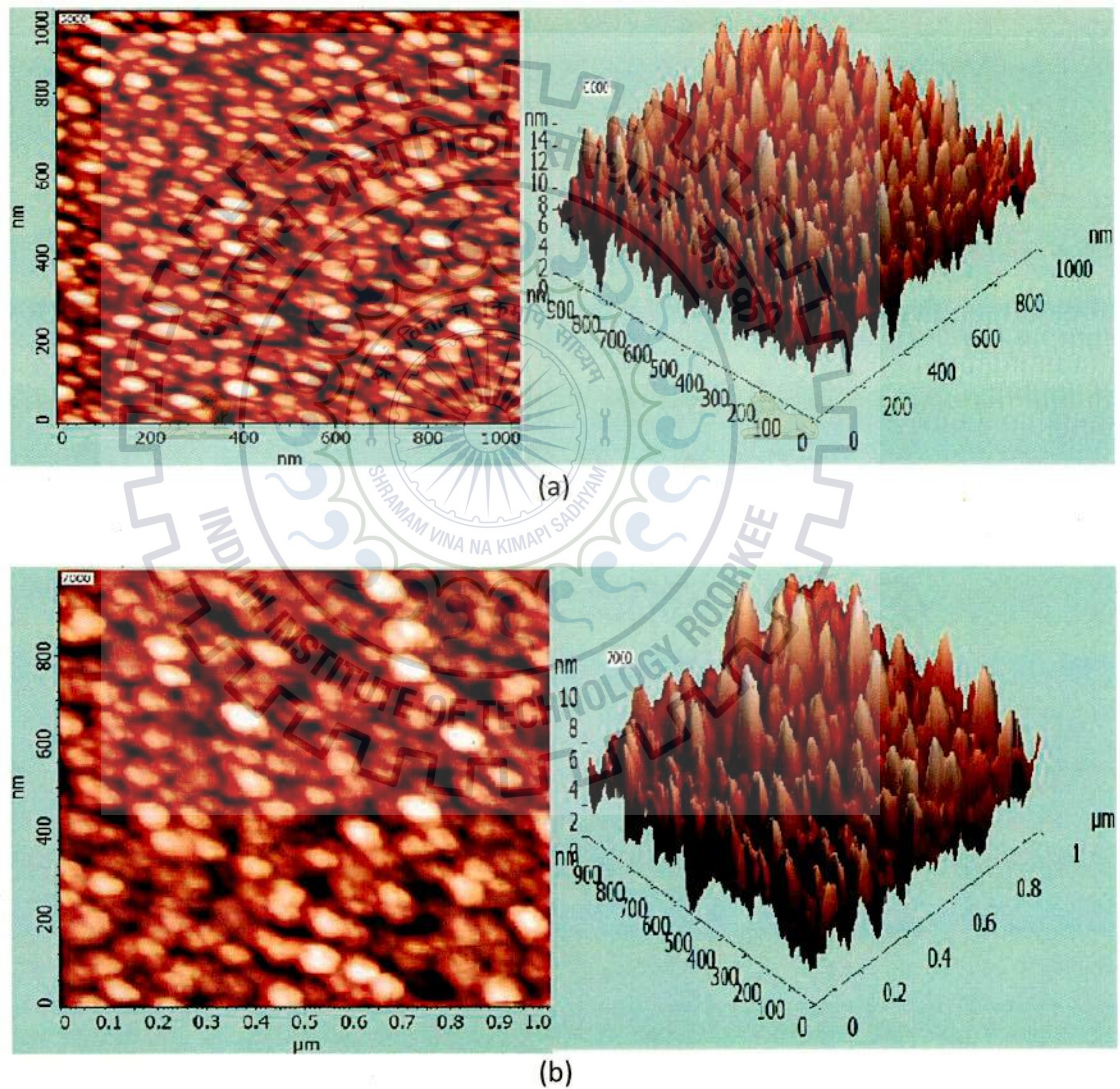


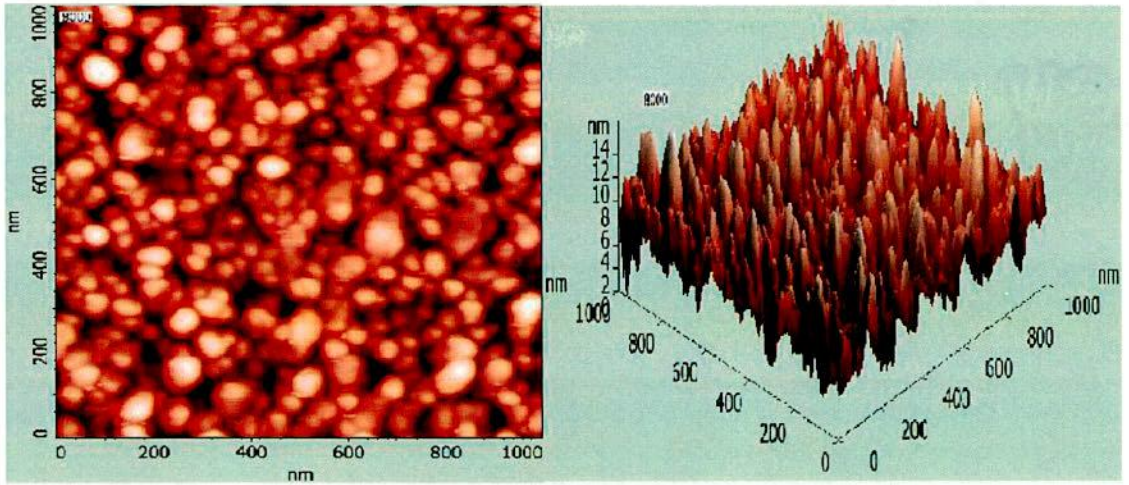
Figure 4.9 Comparison between experimental and theoretical results for 14000 number of pulses film.



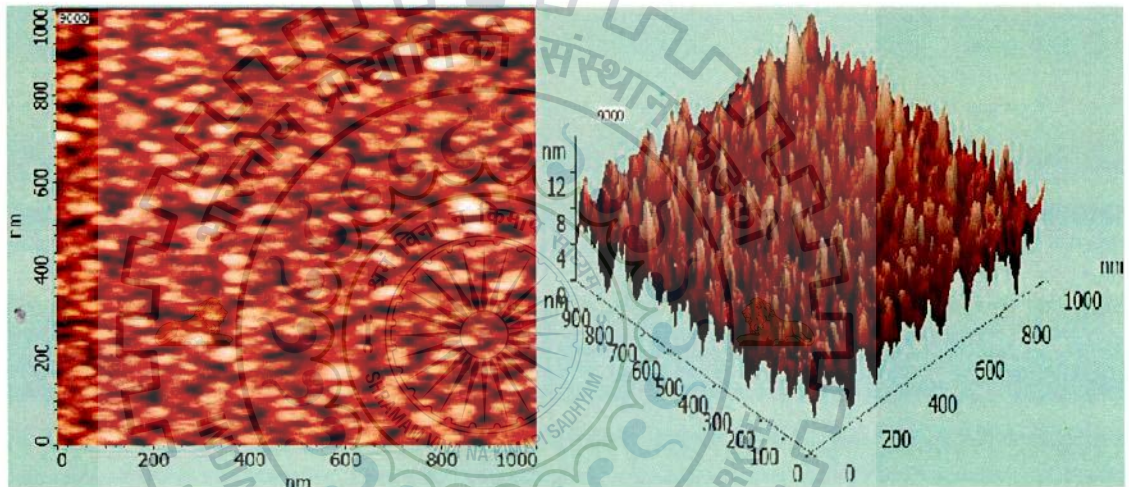
## Morphology of the films

**Figure 4.10** (a)-(g) shows the morphology of the silver film with a scan size ( $1\mu\text{m} \times 1\mu\text{m}$ ). It is deposited on glass substrate at 355nm laser wavelength, grown at room temperature and fabricated by pulsed laser deposition system at 6cm target to substrate distance (TSD). **Figure 4.10** shows an AFM images for the film deposited with 6000, 7000, 8000, 9000, 10000, 12000 & 14000 number of pulses.

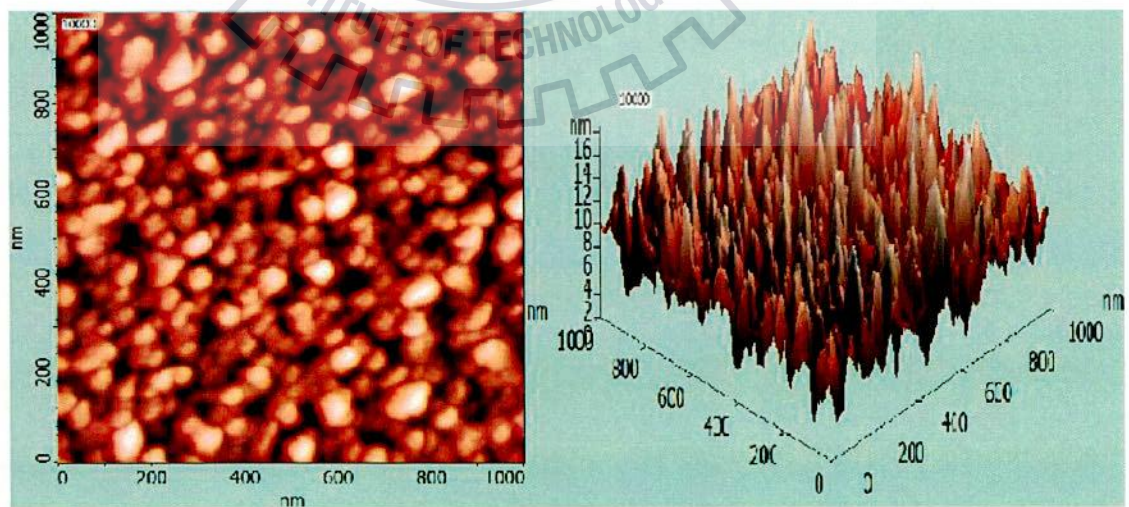




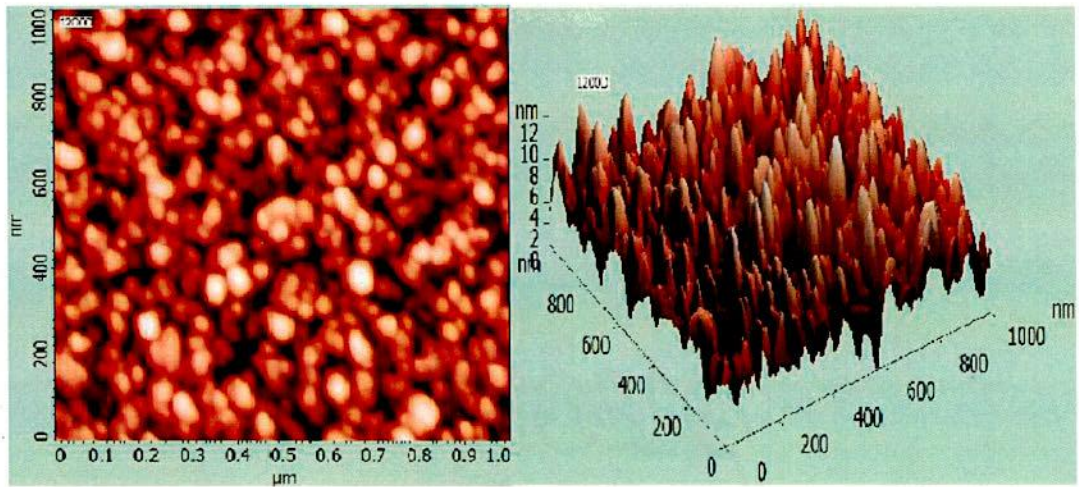
(c)



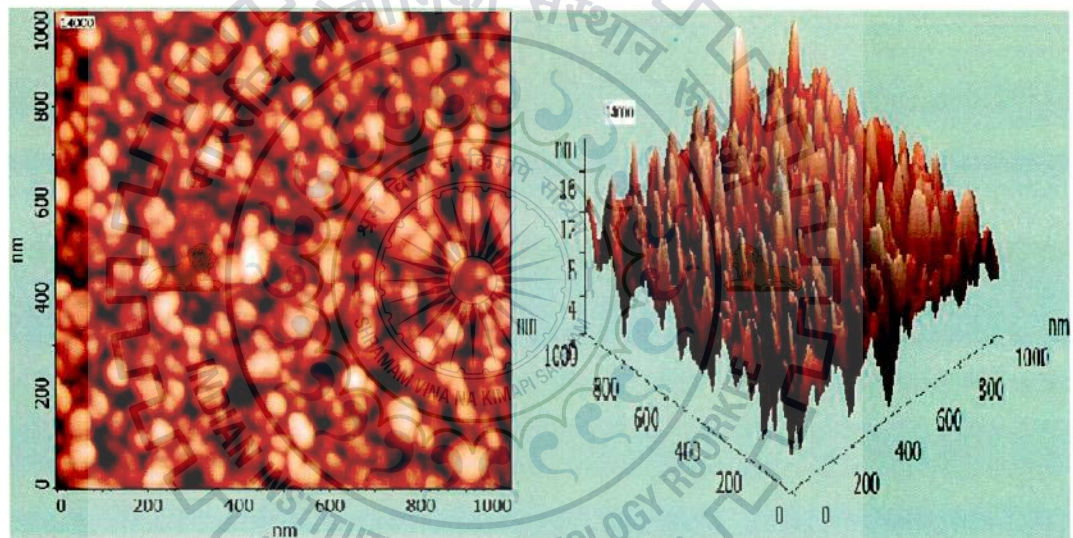
(d)



(e)



(f)



(g)

**Figure 4.10 (a)-(g)** AFM images  $1 \times 1 \mu\text{m}^2$  of nano structured silver thin films of 355nm of laser wavelength with their 3-D images of different no. of pulses at room temperature (a)6000 (b)700 (c)8000 (d)9000 (e)10000 (f)12000 (g)14000 number of pulses.

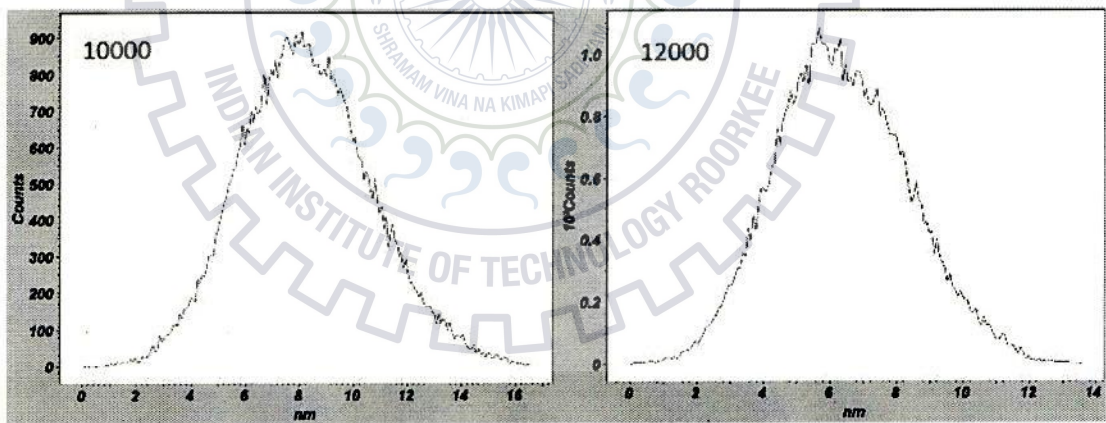
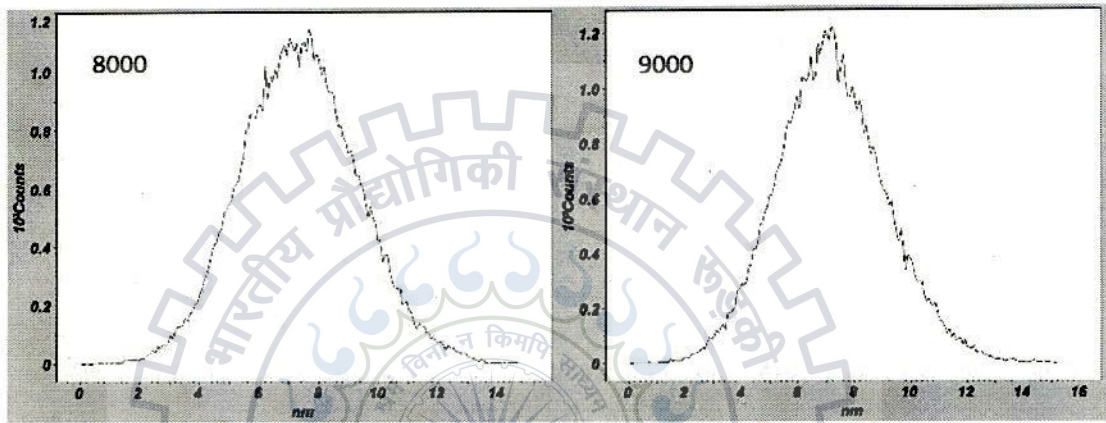
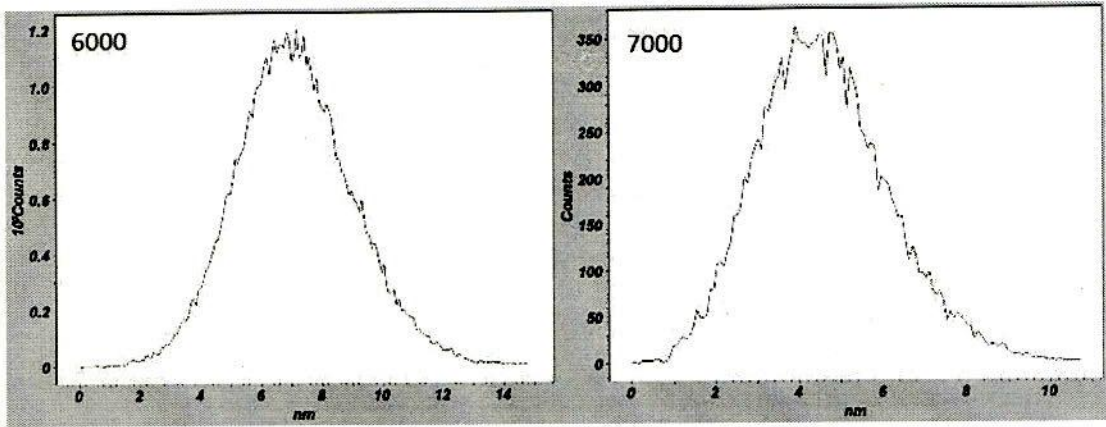
The film deposited with 6000, 7000, 8000, 9000 number of pulses shows a ellipsoidal particle shape whereas deposited with 10000, 12000 & 14000 number of pulses shows a spherical particle shape nature. The size of silver (Ag) nanoparticle is increasing as the

number of pulses increases or we can say that as the thickness increasing the size of silver (Ag) nanoparticle is increasing as shown in Table 1. From the AFM analysis the average roughness of silver deposited film are decreasing with increasing number of pulses as shown in Table 1.

**Table 1**

355nm laser wavelength films (number of pulses)	Particle size(nm)	Average roughness (nm)
6000	5.352	2.513
7000	6.760	2.423
8000	7.434	1.990
9000	7.515	1.954
10000	7.966	1.935
12000	8.252	1.917
14000	9.601	1.558

The performance of surface plasmons resonance is strongly affected by the roughness of the metal film, Narrow dip is obtained with a smooth surface whereas a broad dip is obtained with a rough surface of the metal film from figure 4.10 it is analyse that broad dip is occur in 6000, 7000, 8000, 9000 number of pulses film due to the rough surface of the metal film whereas narrow dip is obtained in 10000, 12000 & 14000 number of pulses film due to the smooth surface.



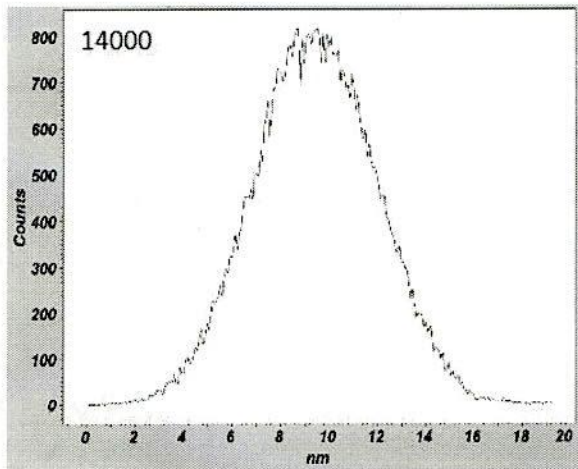


**Figure 4.11** Histogram of AFM shows distribution of particle size of different thickness of silver thin films of 355nm of laser wavelength at room.

The distribution of particle size of silver film of different thickness are shown in histogram **figure 4.11** from this figure we analyse that the particle size distribution in 6000, 7000, 8000, 9000 number of pulses film is less as compared with particle size distribution in 10000, 12000 & 14000 number of pulses films. This result shows that with the increasing number of pulses, particle size distribution is increasing as particle shape is changing.

## Conclusion

Preparation and characterization of different thickness of silver (Ag) thin films on to a glass substrate for Surface Plasmon resonance (SPR) measurement were performed. Surface plasmons resonance is very sensitive to the incident angle near the resonance angle that can be used to sense different refractive indices. The characterization of different thickness in the range of 6000 - 14000 numbers of pulses of Ag film has been studied by the help of SPR technique in the kretschmann configuration and morphology study by AFM. The surface Plasmon resonance occurs at wavelength in the visible and near infrared region of the EM spectrum. We see that with the increasing incident angle beyond the critical angle dip of reflectivity occur with the increasing number of pulses shifting of surface plasmons resonance occurs. The current results shows that the SPR technique is used for studying the optical properties of different thickness of Ag films and by morphological analysis we get the structural analysis depend on the thickness of the film due to this wide reflectance dip is obtained for rough surface where as narrow dip is obtained for smooth surface & particle shape, size and height depends on the thickness of the metal film this highlight the application for various sensors such as chemical and biological sensors etc.



## References

- [1] C. Kittel, 7th. ed. Wiley, New York (1996).
- [2] S. Kawata, Ed., Topics in Appl. Phys. 81, Springer-Verlag, Berlin (2001).
- [3] V. M. Agranovich and D. L. Mills, eds., (North-Holland, 1982).
- [4] B. Liedberg, C. Nylander and I. Lundstrum, Sens. Actuators B 4, 299 (1983).
- [5] L. M. Zhang and D. Uttamchandani, Electron. Lett. 23, 1469 (1988).
- [6] J. Homola, S. S. Yee and G. Gauglitz, Sens. Actuators B 54, 3 (1999).
- [7] N. Pryds, J. Schou, and S. Linderoth, Appl. Surf. Sci. 253, 8231 (2007).
- [8] F. K. Shan and Y. S. Yu, Thin Solid Films 435, 174 (2003).
- [9] K. Hasegawa, K. Fujino, H. Mukai, M. Konishi, K. Hayashi, K. Sato, S. Honjo, Y. Sato, H. Ishii, and Y. Iwata, Applied Superconductivity 4, 487 (1996).
- [10] B. Mayor, J. Arias, and S. Chiussi, Thin Solid Films 317, 363 (1998).
- [11] P. I. Nikitin, A. A. Beloglazov, A. Y. Toporov, M. V. Valeiko, V. I. Konov, A. Perrone, A. Luches, L. Mirengi, and L. Tapfer, J. Appl. Phys. 82, 1408 (1997).
- [12] A. Peterlongo, A. Miotello, and R. Kelly, Phys. Rev. E 50, 4716 (1994).
- [24] Sommerfeld, A. Fortpflanzung elektrodynamischer Wellen an einem zylindrischen Leiter, Ann. der Physik und Chemie (1899), 67, 233
- [25] Drude, P. Zur Elektronentheorie der metalle, Ann. Phys. (1900), 306, 3, 566
- [26] Drude, P. Zur Elektronentheorie der Metalle: II. Teil. Galvanomagnetische und thermomagnetische Effecte, Ann. Phys. (1900), 308, 11, 369
- [27] Tonks, L.; Langmuir, I. Oscillations in Ionized Gases, Phys. Rev. (1929), 33, 195.
- [28] Raether, H. Surface Plasmons, Springer-Verlag, Berlin (1998)

- [29] Sambles, J. R.; Bradbery, G. W.; Yang, F. Z. Optical-excitation of surface plasmons - an introduction, *Contemp. Phys.* (1991), 32, 173
- [30] Max Born and Emil Wolf. *Principles of Optics*. Pergamon Press, 6<sup>th</sup> corrected ed., reprinted edition, (1984).
- [31] M. C. Hutley. *Diffraction gratings*. Academic Press, London, (1982).
- [32] Kaufmann, E.N. *Characterization of materials*, John Wiley & sons, 2003.
- [33] Shirley, D.A. *Phys. Rev. B* 1972, 5, 4709.
- [34] G Binnig, C F Quate, C Gerber, Atomic force microscope, *Phys. Rev. Lett.*, Vol. 56, No.9, pp.930–933, 1986.
- [35] Reather H, Surface plasmons on smooth and rough surfaces and on grating, *Springer Tracts in Modern Physics*, Vol.111, 1988, chap.2.
- [36] Jir'í Homola†, *Surface Plasmon Resonance Sensors for Detection of Chemical and Biological Species*.